Velocity-dependent dark matter annihilation from simulations

Nassim Bozorgnia

UNIVERSITY OF ALBERTA

In collaboration with E. Piccirillo, L. Strigari and Auriga & APOSTLE groups

arXiv: 2101.06284, 2203.08853, 2207.00069

TeVPA 2022, Queen's University, 11 August 2022

Galactic dark matter distribution

Signals in indirect DM searches strongly depend on the DM distribution in the Milky Way.

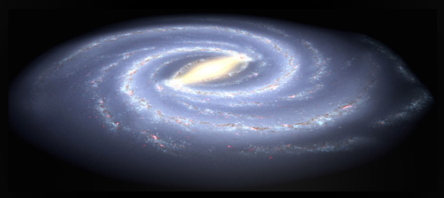

Galactic dark matter distribution

Signals in indirect DM searches strongly depend on the DM distribution in the Milky Way.

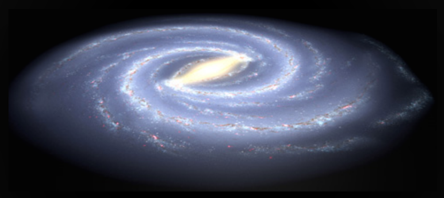

Use high resolution cosmological simulations to extract the Galactic DM distribution and study the implications for velocity-dependent DM annihilation.

Velocity-independent annihilation

- In the **s-wave annihilation** model, the DM annihilation cross section is *velocity-independent*, and the expected gamma-ray flux from DM annihilation is:

$$\frac{d\Phi_\gamma}{dE} = \frac{\langle \sigma_A v_{\rm rel} \rangle}{8\pi m_\chi^2} \frac{dN_\gamma}{dE} \int_{\rm l.o.s} d\ell \; [\rho(r(\ell, \Psi))]^2$$

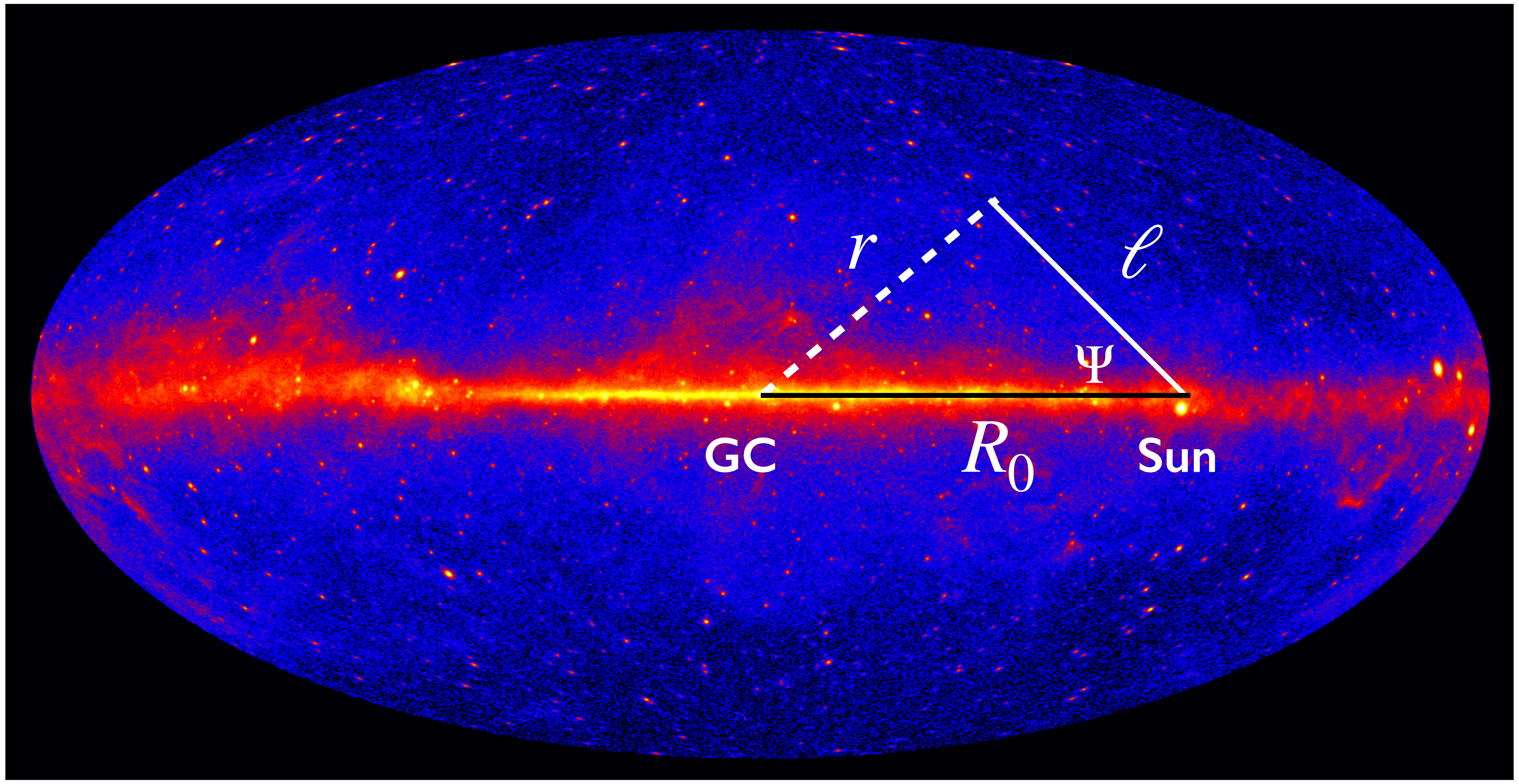

Velocity-independent annihilation

- In the **s-wave annihilation** model, the DM annihilation cross section is *velocity-independent*, and the expected gamma-ray flux from DM annihilation is:

astrophysics

$\mathcal{J}$- factor

$$\frac{d\Phi_\gamma}{dE} = \frac{\langle \sigma_A v_{\rm rel} \rangle}{8\pi m_\chi^2} \frac{dN_\gamma}{dE} \int_{\rm l.o.s} d\ell \, [\rho(r(\ell, \Psi))]^2$$

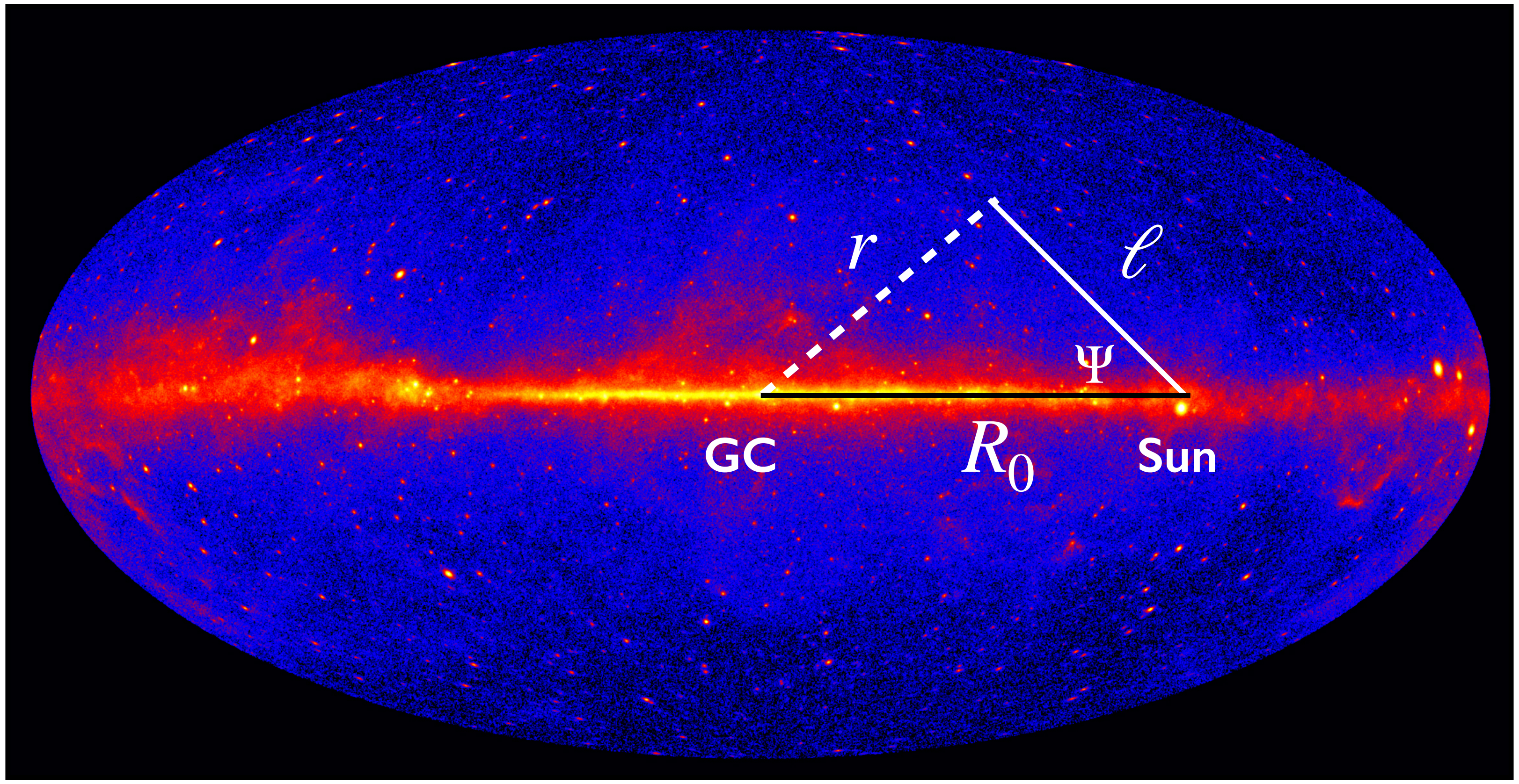

Velocity-dependent annihilation

- For *velocity-dependent* models, the J-factor must also include the DM pair-wise relative velocity distribution.

Velocity-dependent annihilation

- For *velocity-dependent* models, the J-factor must also include the DM pair-wise relative velocity distribution.

- The annihilation cross section averaged over the relative velocity distribution is defined as:

$$\langle \sigma_A v_{\rm rel} \rangle (\mathbf{x}) = \int \mathrm{d}^3\mathbf{v}_{\rm rel} P_{\mathbf{x}}(\mathbf{v}_{\rm rel})(\sigma_A v_{\rm rel})$$

DM relative velocity distribution at position $\mathbf{x}$ in the halo

Velocity-dependent annihilation

- For *velocity-dependent* models, the J-factor must also include the DM pair-wise relative velocity distribution.

- The annihilation cross section averaged over the relative velocity distribution is defined as:

$$\langle \sigma_A v_{\rm rel} \rangle (\mathbf{x}) = \int \mathrm{d}^3 \mathbf{v}_{\rm rel} P_{\mathbf{x}}(\mathbf{v}_{\rm rel}) (\sigma_A v_{\rm rel})$$

DM relative velocity distribution at position $\mathbf{x}$ in the halo

- Parametrize $\sigma_A v_{\rm rel}$ in the general form:

$$\sigma_A v_{\rm rel} = (\sigma_A v_{\rm rel})_0 (v_{\rm rel}/c)^n$$

velocity-independent component of the cross section

Velocity-dependent annihilation

- For *velocity-dependent* models, the J-factor must also include the DM pair-wise relative velocity distribution.

- The annihilation cross section averaged over the relative velocity distribution is defined as:

$$\langle \sigma_A v_{\rm rel} \rangle (\mathbf{x}) = \int \mathrm{d}^3 \mathbf{v}_{\rm rel} P_{\mathbf{x}}(\mathbf{v}_{\rm rel}) (\sigma_A v_{\rm rel})$$

$P_{\mathbf{x}}$ → DM relative velocity distribution at position $\mathbf{x}$ in the halo

- Parametrize $\sigma_A v_{\rm rel}$ in the general form:

$$\sigma_A v_{\rm rel} = (\sigma_A v_{\rm rel})_0 (v_{\rm rel}/c)^n$$

$(\sigma_A v_{\rm rel})_0$ → velocity-independent component of the cross section

Different annihilation models:

- $n = 0$: **s-wave**
- $n = 2$: **p-wave**
- $n = 4$: **d-wave**
- $n = -1$: **Sommerfeld-enhanced**

Velocity-dependent annihilation

- The expected gamma-ray flux from DM annihilation:

$$\frac{d\Phi_\gamma}{dE} = \frac{(\sigma_A v_{\rm rel})_0}{8\pi m_\chi^2} \frac{dN_\gamma}{dE} \, \mathcal{J}_s$$

written in terms of the **effective J-factor**:

$$\mathcal{J}_s(\Psi) = \int d\ell \, \frac{\langle \sigma_A v_{\rm rel} \rangle}{(\sigma_A v_{\rm rel})_0} \left[\rho(r(\ell, \Psi))\right]^2$$

Velocity-dependent annihilation

- The expected gamma-ray flux from DM annihilation:

$$\frac{d\Phi_\gamma}{dE} = \frac{(\sigma_A v_{\rm rel})_0}{8\pi m_\chi^2} \frac{dN_\gamma}{dE} \, \mathcal{J}_s$$

written in terms of the **effective J-factor**:

$$\mathcal{J}_s(\Psi) = \int d\ell \, \frac{\langle \sigma_A v_{\rm rel} \rangle}{(\sigma_A v_{\rm rel})_0} \, [\rho(r(\ell, \Psi))]^2$$

$$= \int d\ell \int d^3\mathbf{v}_{\rm rel} P_{\mathbf{x}}(\mathbf{v}_{\rm rel}) \, \left(\frac{v_{\rm rel}}{c}\right)^n \, [\rho(r(\ell, \Psi))]^2$$

Velocity-dependent annihilation

- The expected gamma-ray flux from DM annihilation:

$$\frac{d\Phi_\gamma}{dE} = \frac{(\sigma_A v_{\rm rel})_0}{8\pi m_\chi^2} \frac{dN_\gamma}{dE} \mathcal{J}_s$$

written in terms of the **effective J-factor**:

$$\mathcal{J}_s(\Psi) = \int d\ell \, \frac{\langle \sigma_A v_{\rm rel} \rangle}{(\sigma_A v_{\rm rel})_0} \left[\rho(r(\ell, \Psi))\right]^2$$

$$= \int d\ell \int d^3\mathbf{v}_{\rm rel} P_{\mathbf{x}}(\mathbf{v}_{\rm rel}) \left(\frac{v_{\rm rel}}{c}\right)^n \left[\rho(r(\ell, \Psi))\right]^2$$

Velocity-dependent annihilation

- The expected gamma-ray flux from DM annihilation:

$$\frac{d\Phi_\gamma}{dE} = \frac{(\sigma_A v_{\rm rel})_0}{8\pi m_\chi^2} \frac{dN_\gamma}{dE} \mathcal{J}_s$$

written in terms of the **effective J-factor**:

$$\mathcal{J}_s(\Psi) = \int d\ell \, \frac{\langle \sigma_A v_{\rm rel} \rangle}{(\sigma_A v_{\rm rel})_0} \left[\rho(r(\ell,\Psi))\right]^2$$

$$= \int d\ell \int d^3\mathbf{v}_{\rm rel} P_{\mathbf{x}}(\mathbf{v}_{\rm rel}) \left(\frac{v_{\rm rel}}{c}\right)^n \left[\rho(r(\ell,\Psi))\right]^2$$

$$= \int d\ell \left[\rho(r(\ell,\Psi))\right]^2 \left(\frac{\mu_n(\mathbf{x})}{c^n}\right)$$

Velocity-dependent annihilation

- The expected gamma-ray flux from DM annihilation:

$$\frac{d\Phi_\gamma}{dE} = \frac{(\sigma_A v_{\rm rel})_0}{8\pi m_\chi^2}\frac{dN_\gamma}{dE}\,\mathcal{J}_s$$

written in terms of the **effective J-factor**:

$$\mathcal{J}_s(\Psi) = \int d\ell\,\frac{\langle\sigma_A v_{\rm rel}\rangle}{(\sigma_A v_{\rm rel})_0}\,[\rho(r(\ell,\Psi))]^2$$

$$= \int d\ell \int d^3\mathbf{v}_{\rm rel} P_{\mathbf{x}}(\mathbf{v}_{\rm rel})\,\left(\frac{v_{\rm rel}}{c}\right)^n\,[\rho(r(\ell,\Psi))]^2$$

$$= \int d\ell\,[\rho(r(\ell,\Psi))]^2\left(\frac{\mu_n(\mathbf{x})}{c^n}\right)$$

- Different annihilation models correspond to different ***moments*** of the relative velocity distribution.

Velocity-dependent annihilation

- The expected gamma-ray flux from DM annihilation:

$$\frac{d\Phi_\gamma}{dE} = \frac{(\sigma_A v_{\rm rel})_0}{8\pi m_\chi^2}\frac{dN_\gamma}{dE}\,\mathcal{J}_s$$

Extract the DM distribution (of the smooth halo) from simulated Milky Way-like galaxies in **Auriga** and **APOSTLE**.

$$= \int d\ell \int d^3\mathbf{v}_{\rm rel} P_{\mathbf{x}}(\mathbf{v}_{\rm rel}) \left(\frac{v_{\rm rel}}{c}\right)^n [\rho(r(\ell,\Psi))]^2$$

$$= \int d\ell\, [\rho(r(\ell,\Psi))]^2 \left(\frac{\mu_n(\mathbf{x})}{c^n}\right)$$

- Different annihilation models correspond to different ***moments*** of the relative velocity distribution.

Hydrodynamical simulations

Auriga Simulations

State-of-the-art magneto-hydrodynamical zoom simulations of Milky Way mass halos.

$m_{\rm DM}$ [$M_\odot$]	$m_{\rm b}$ [$M_\odot$]	ϵ [pc]
3×10^5	5×10^4	369

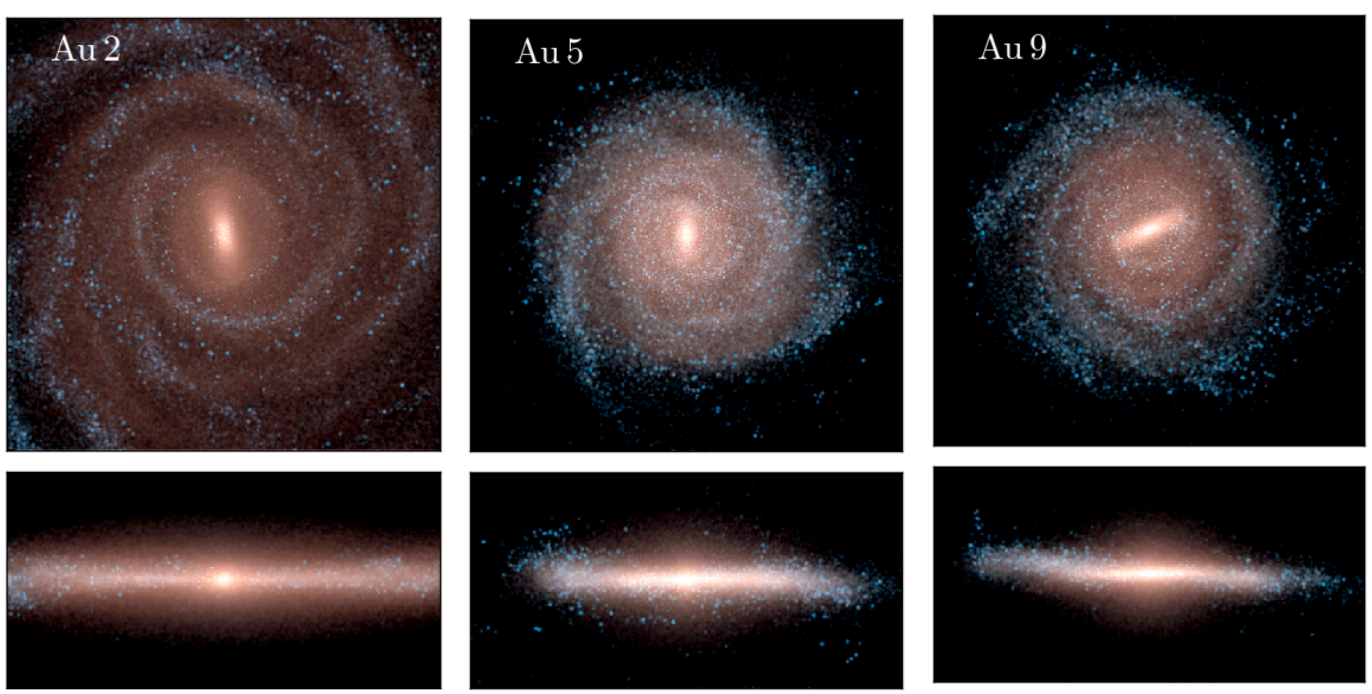

APOSTLE Simulations

Zoom simulations of Local Group analogue systems.

$m_{\rm DM}$ [$M_\odot$]	$m_{\rm b}$ [$M_\odot$]	ϵ [pc]
5.9×10^5	1.3×10^5	308

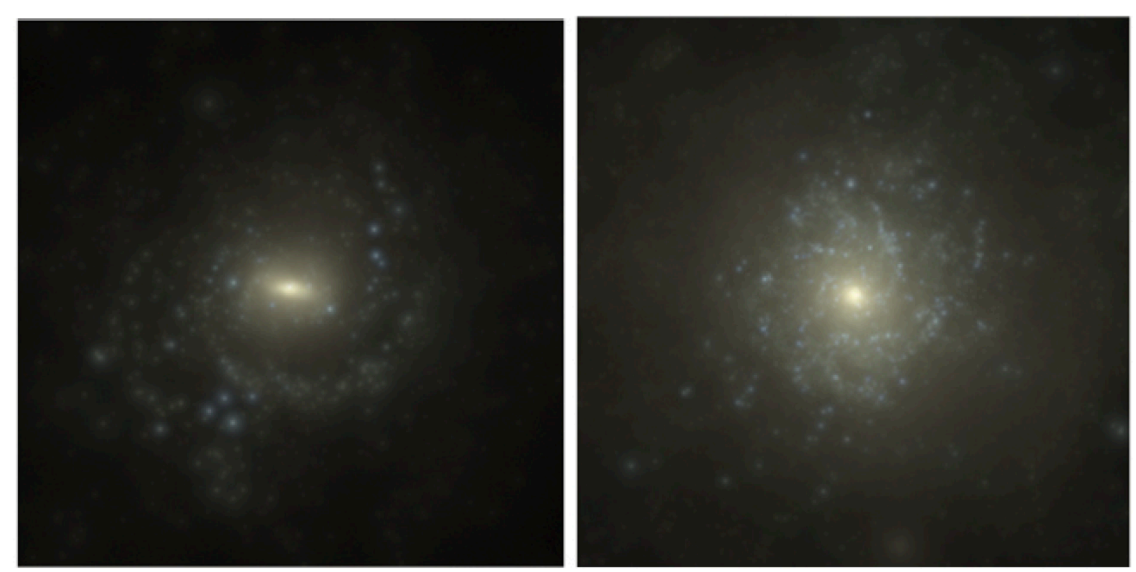

Milky Way analogues

- Identify Milky Way analogues by requiring that **total stellar mass** and **rotation curves** fit observations.

Initial halos:
Auriga: 30
APOSTLE: 24

Milky Way-like:
Auriga: 10
APOSTLE: 6

Halo Name	M_{200} [$\times 10^{12}$ M$_\odot$]	$M_\star$ [$\times 10^{10}$ M$_\odot$]
Au2	1.91	7.65
Au4	1.41	7.54
Au5	1.19	6.88
Au7	1.12	5.27
Au9	1.05	6.20
Au12	1.09	6.29
Au19	1.21	5.72
Au21	1.45	8.02
Au22	0.93	6.10
Au24	1.49	7.07
AP-V1-1-L2	1.64	4.88
AP-V6-1-L2	2.15	4.48
AP-S4-1-L2	1.47	4.23
AP-V4-1-L2	1.26	3.60
AP-V4-2-L2	1.25	3.20
AP-S6-1-L2	0.89	2.41

Dark matter density profiles

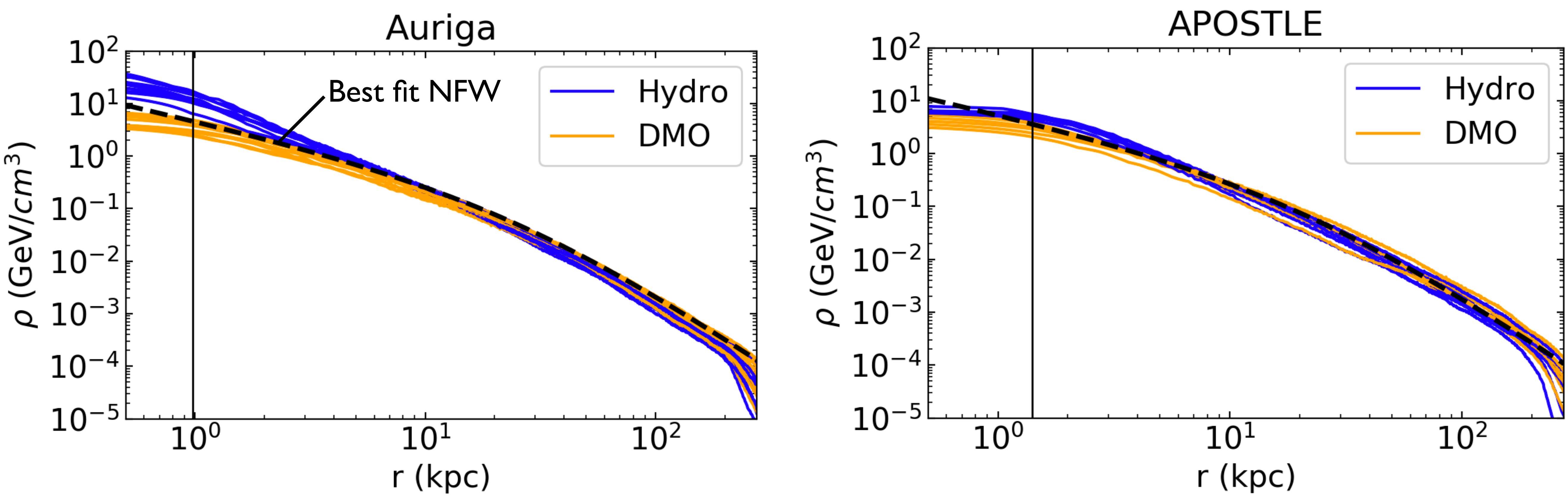

Board, NB, Strigari et al, 2101.06284

Dark matter density profiles

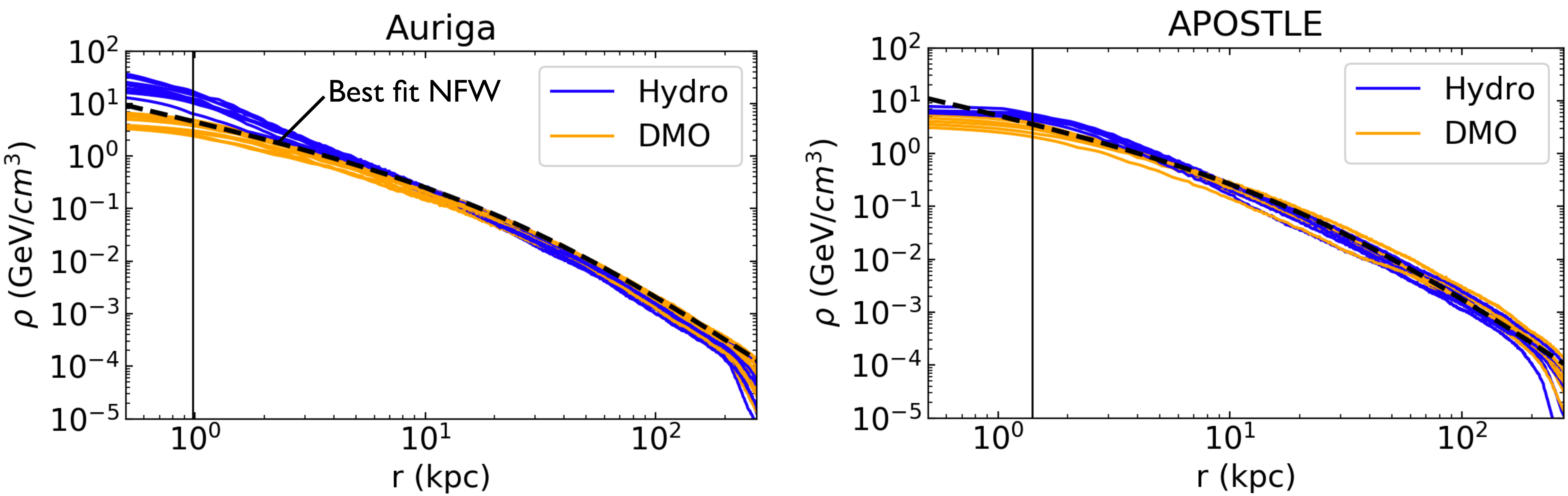

Board, **NB**, Strigari et al, 2101.06284

- At large radii, agreement between hydro and DMO.
- Inside the Solar circle, baryons lead to contraction of the DM halos. → Hydro halos have steeper profiles than DMO.
- APOSTLE halos have smaller stellar masses. → Less contraction of the halos.

DM relative velocity distributions

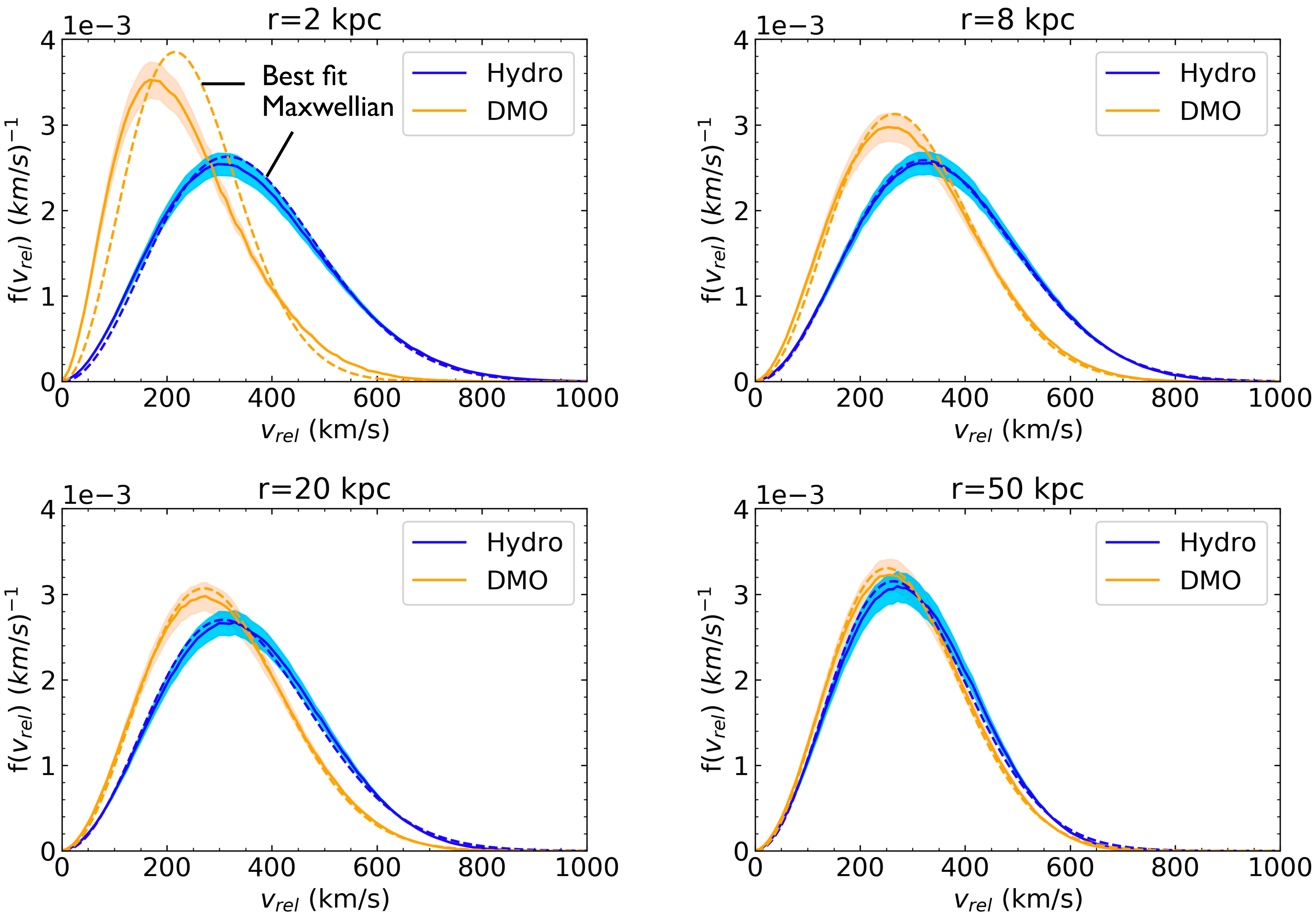

Board, **NB**, Strigari et al, 2101.06284

DM relative velocity distributions

- For the hydro halos, the relative speed distributions are very close to the **Maxwellian distribution** at all radii.
- For the DMO halos, the agreement with the Maxwellian not so good at small radii. → This is because the DM density profiles deviate from the isothermal r^{-2} profile in the central regions of the DMO halos.

Effective J-factors

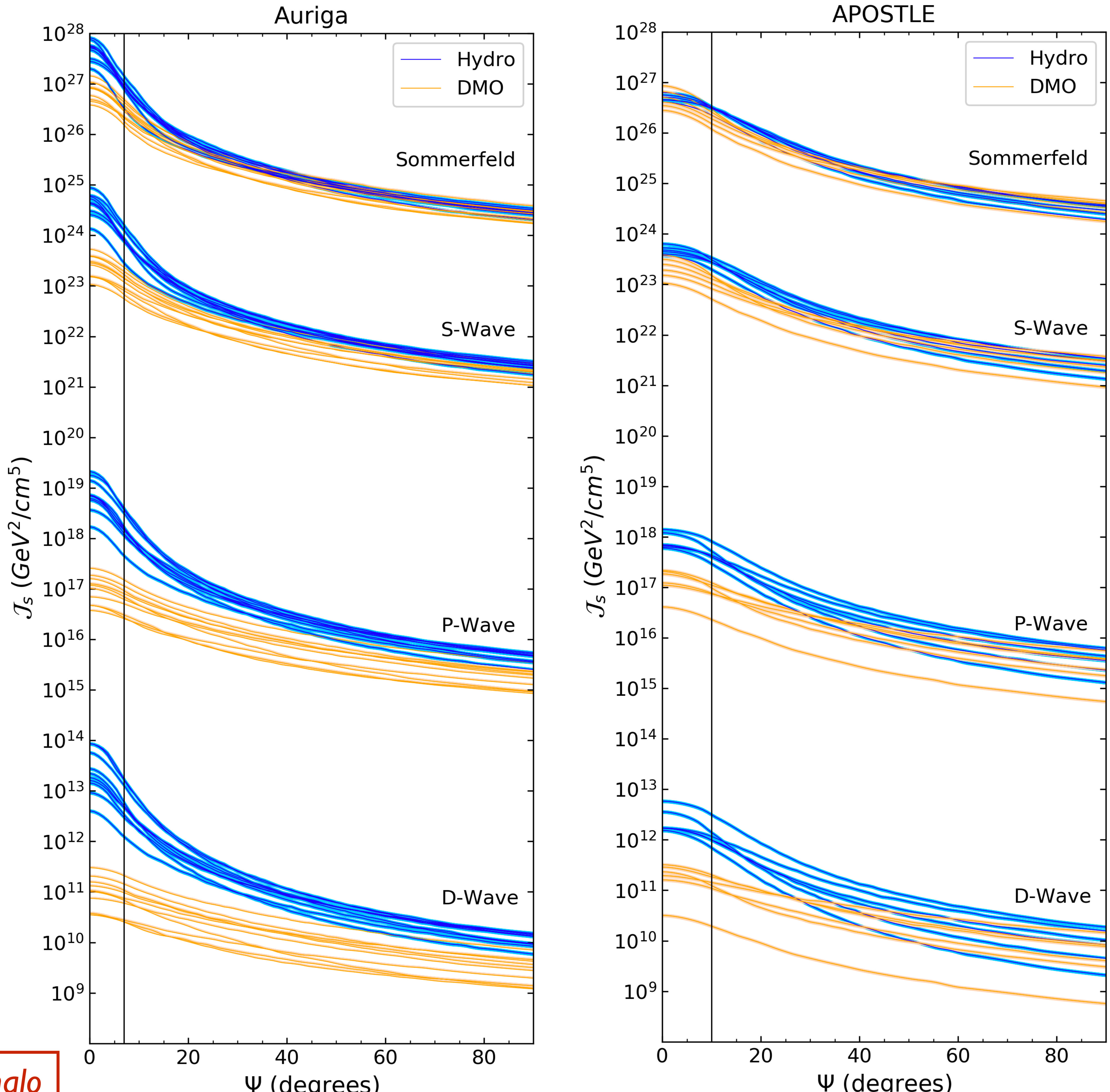

For smooth halo

Board, **NB**, Strigari et al, 2101.06284

Effective J-factors

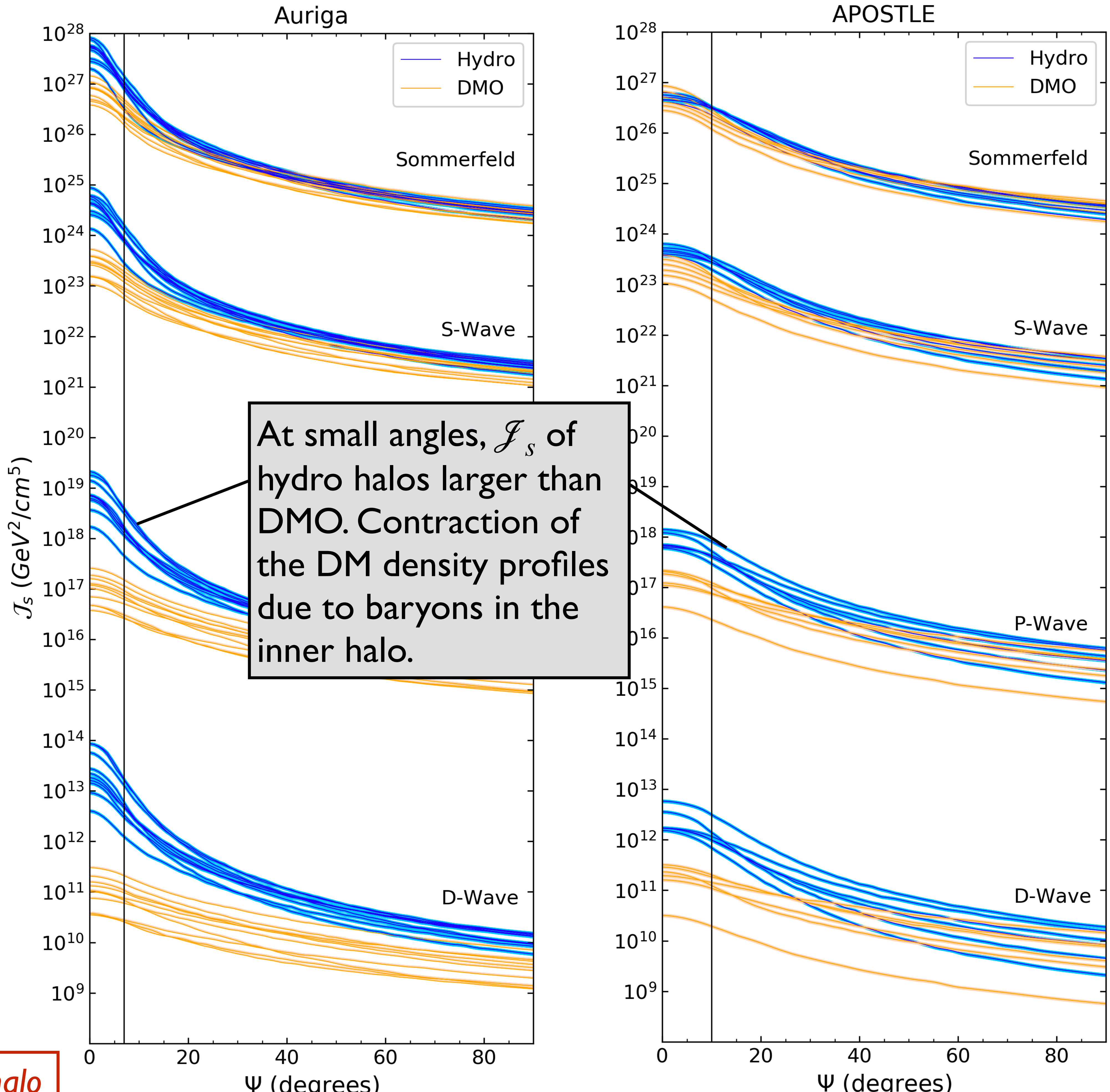

For smooth halo

Board, **NB**, Strigari et al, 2101.06284

Effective J-factors

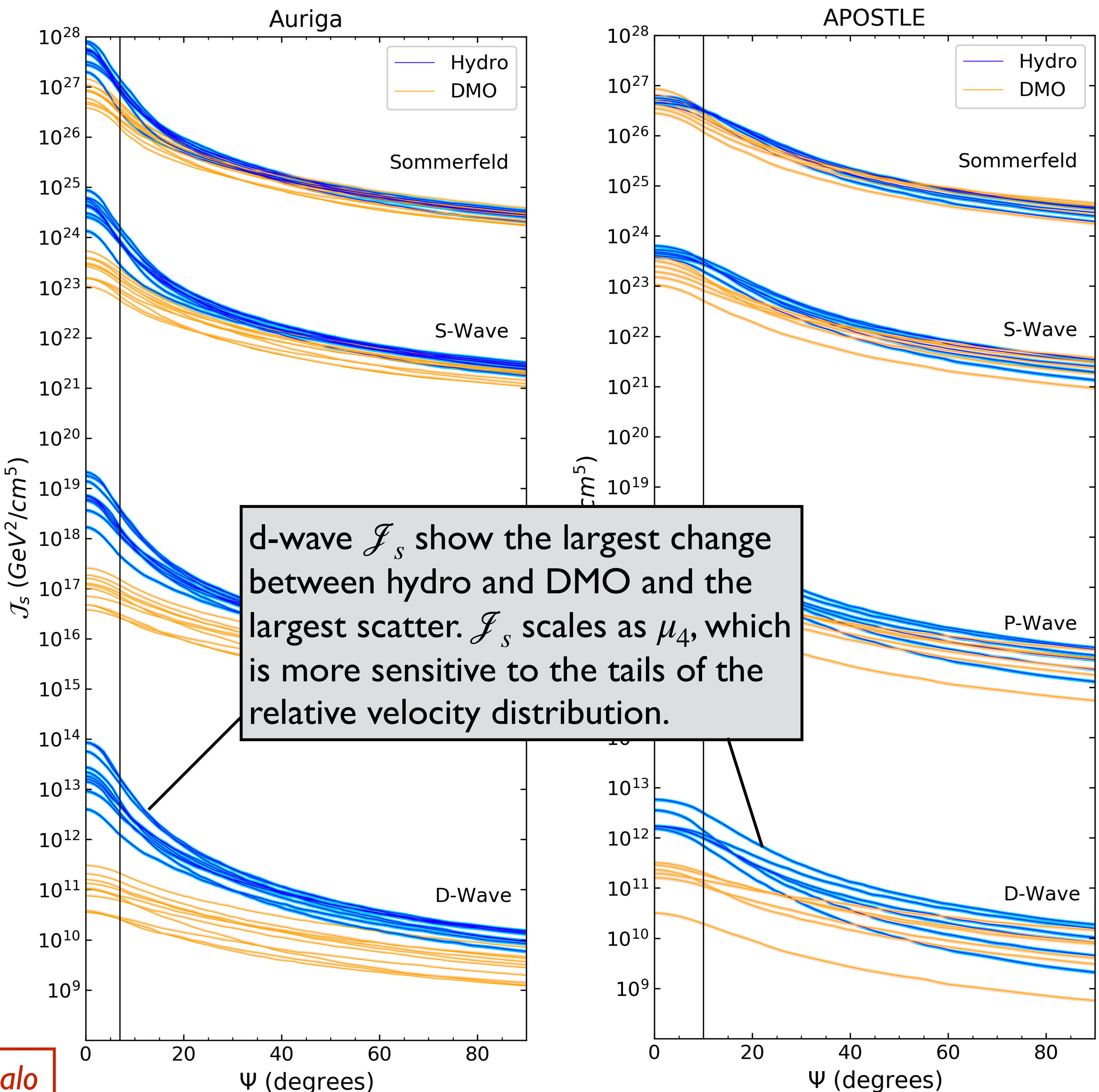

d-wave $\mathcal{J}_s$ show the largest change between hydro and DMO and the largest scatter. $\mathcal{J}_s$ scales as μ_4, which is more sensitive to the tails of the relative velocity distribution.

For smooth halo

Board, **NB**, Strigari et al, 2101.06284

Effective J-factors

- Features in $f(v_{\rm rel})$ explain the differences in the $\mathcal{J}_s$-factors between hydro and DMO halos for each model.

Effective J-factors

- Features in $f(v_{\mathrm{rel}})$ explain the differences in the $\mathcal{J}_s$-factors between hydro and DMO halos for each model.
- The scaling of the $\mathcal{J}_s$ with angle is almost entirely driven by the DM density profiles, and depends very weakly on $f(v_{\mathrm{rel}})$.

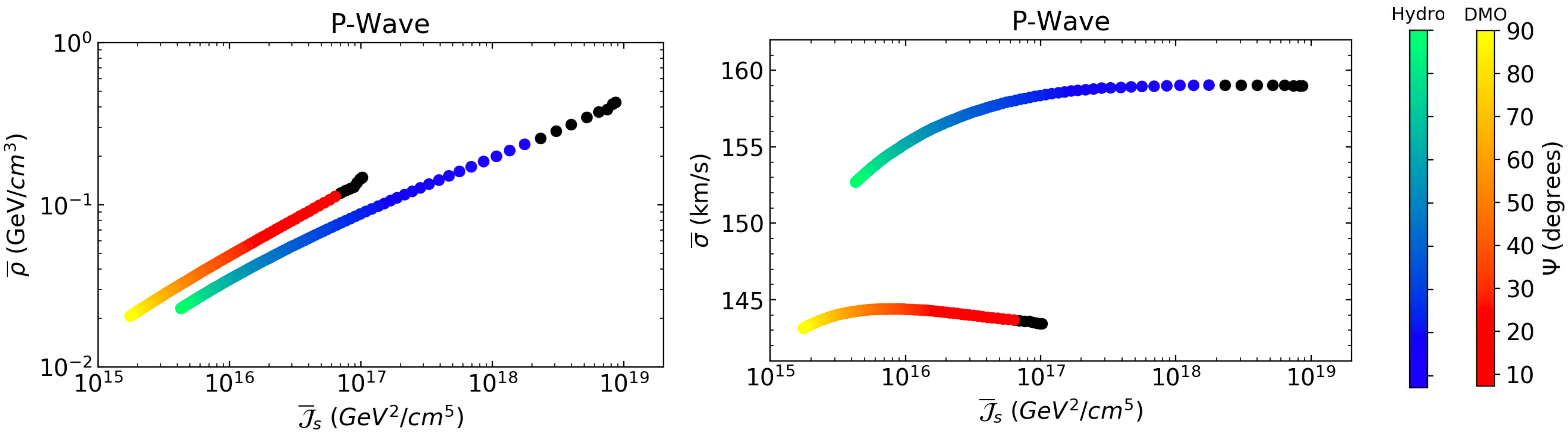

Effective J-factors

- Features in $f(v_{\rm rel})$ explain the differences in the $\mathcal{J}_s$-factors between hydro and DMO halos for each model.

- The scaling of the $\mathcal{J}_s$ with angle is almost entirely driven by the DM density profiles, and depends very weakly on $f(v_{\rm rel})$.

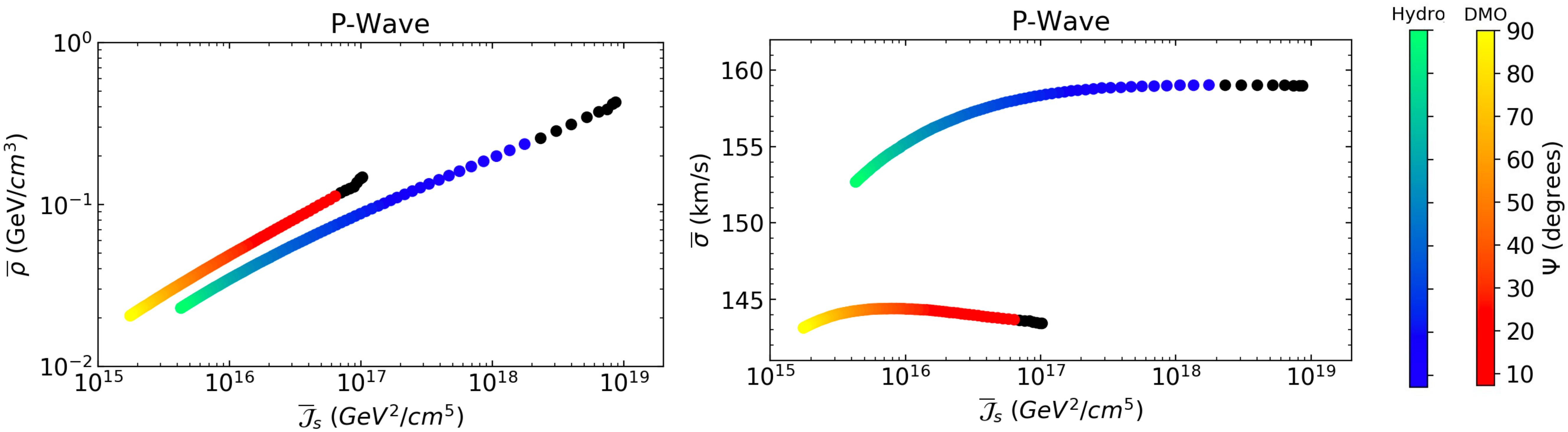

- Understanding the systematics in the DM density profile is the most important factor in determining the $\mathcal{J}_s$-factor.

The impact of subhalos

- For **s-wave**, the boost due to subhalos is small at the resolution limit of current simulations (Auriga high res resolves subhlao mass down to $\sim 10^6\,\mathrm{M}_{\odot}$).

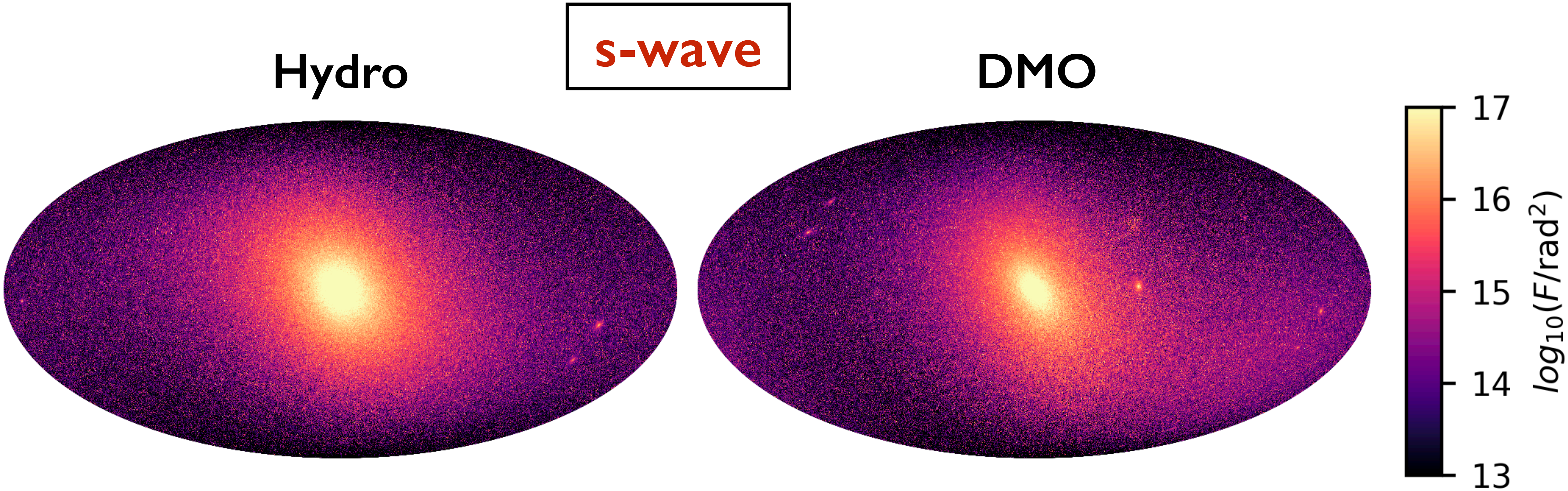

Piccirillo, Blanchette, **NB** et al, 2203.08853

The impact of subhalos

- For **s-wave**, the boost due to subhalos is small at the resolution limit of current simulations (Auriga high res resolves subhlao mass down to $\sim 10^6\,\mathrm{M}_{\odot}$).

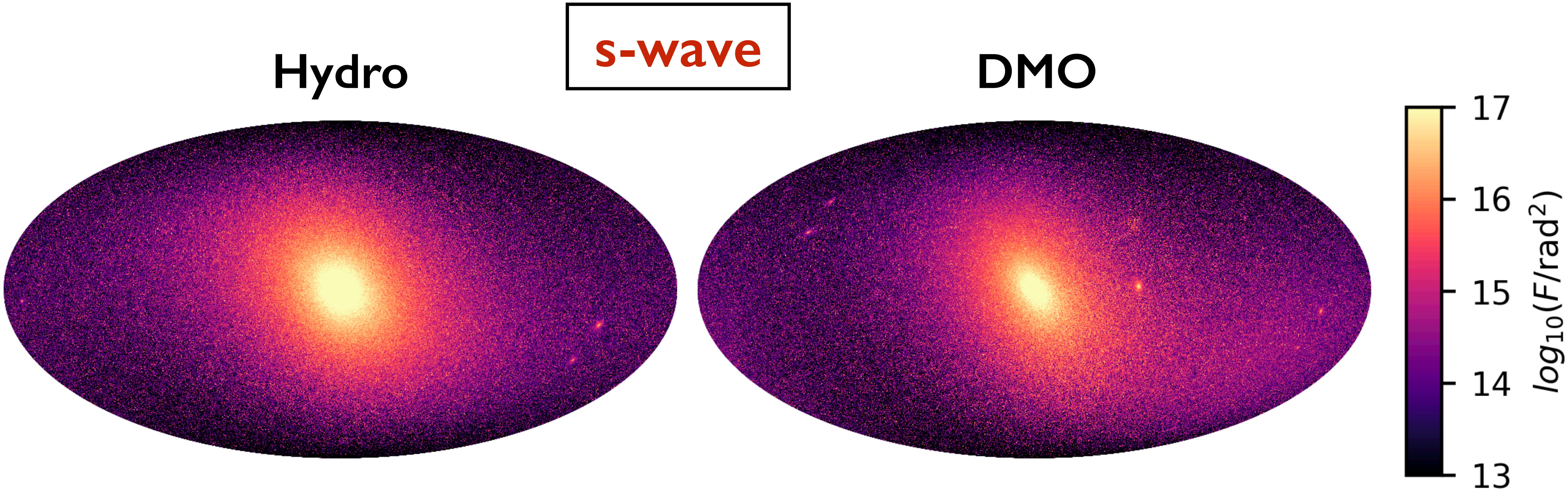

Piccirillo, Blanchette, **NB** et al, 2203.08853

- In the hydro halos, subhalo fluxes are fainter and the smooth component is brighter and rounder compared to DMO.

The impact of subhalos

- For **p-wave** and **d-wave**, DM annihilation fluxes from subhalos are suppressed relative to the smooth halo.

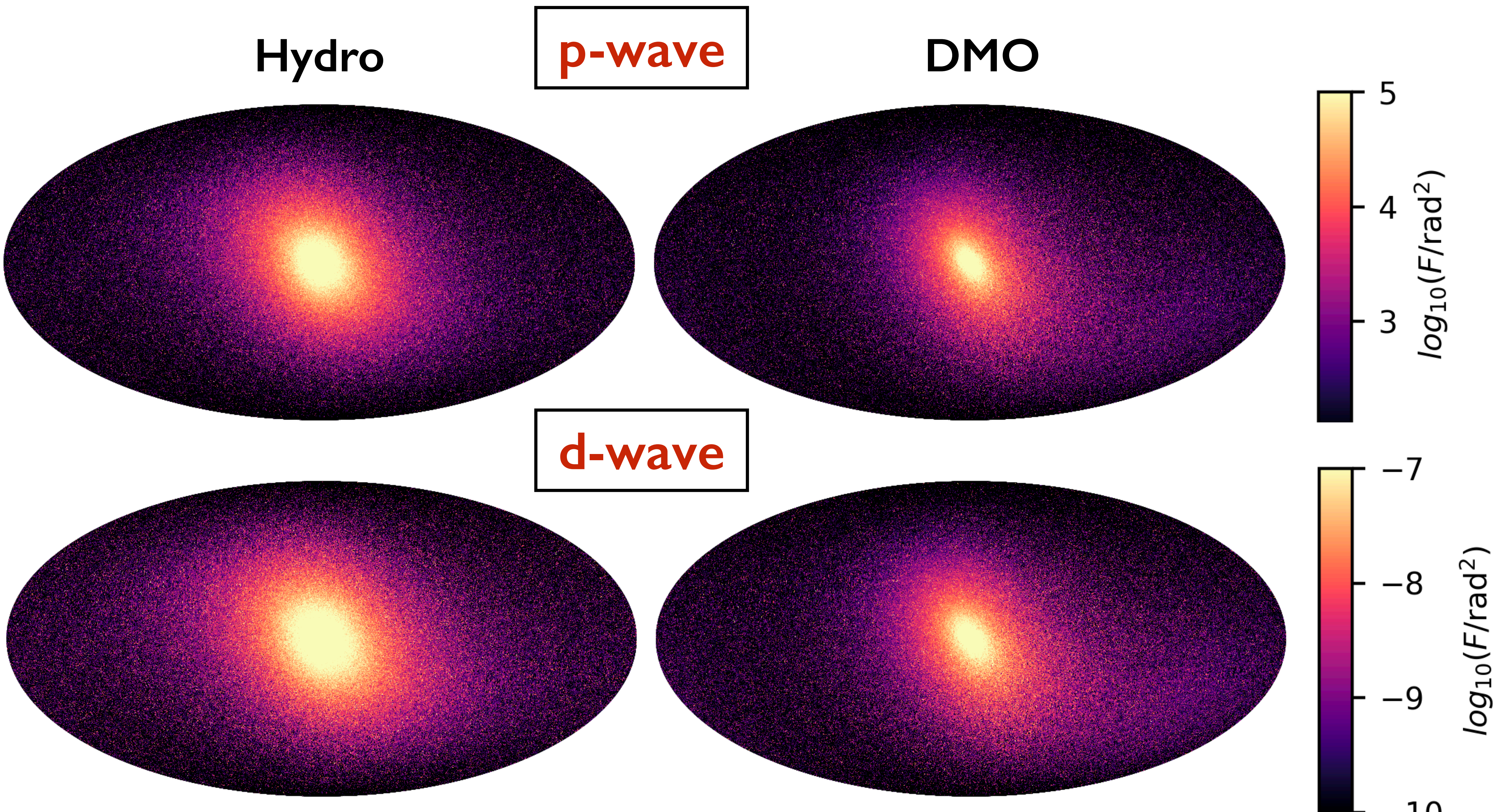

Piccirillo, Blanchette, **NB** et al, 2203.08853

The impact of subhalos

- Contribution from subhalos most significant in **Sommerfeld** models, where it dominates the smooth component beyond $\sim 0.74\, r_{200}$.

Sommerfeld

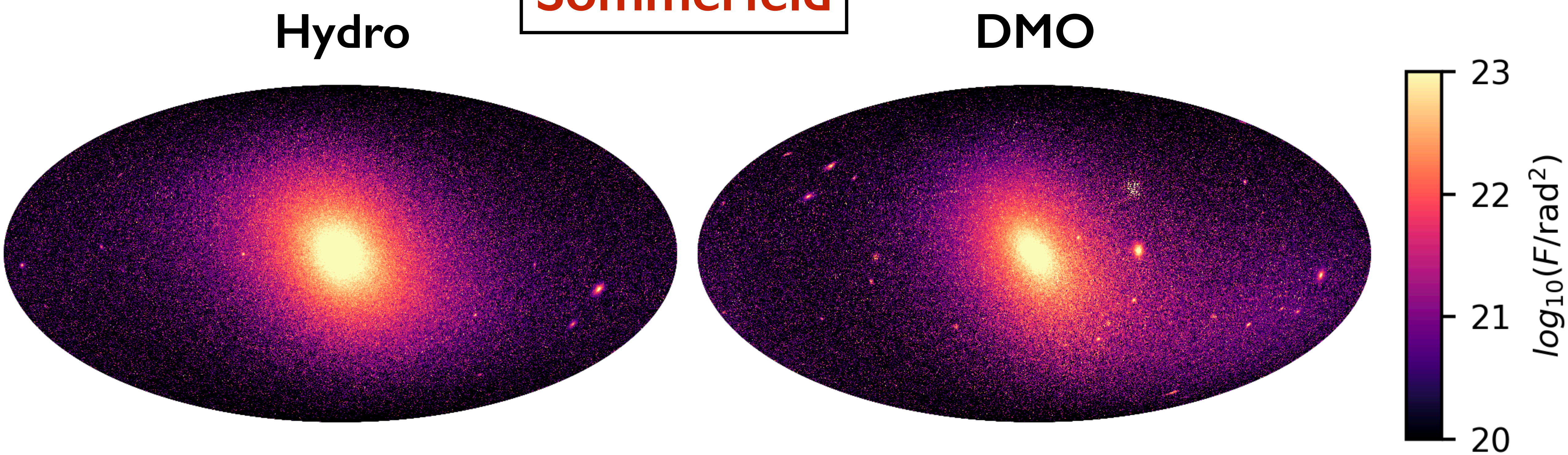

Piccirillo, Blanchette, **NB** et al, 2203.08853

The impact of subhalos

- Contribution from subhalos most significant in **Sommerfeld** models, where it dominates the smooth component beyond $\sim 0.74\, r_{200}$.

Sommerfeld

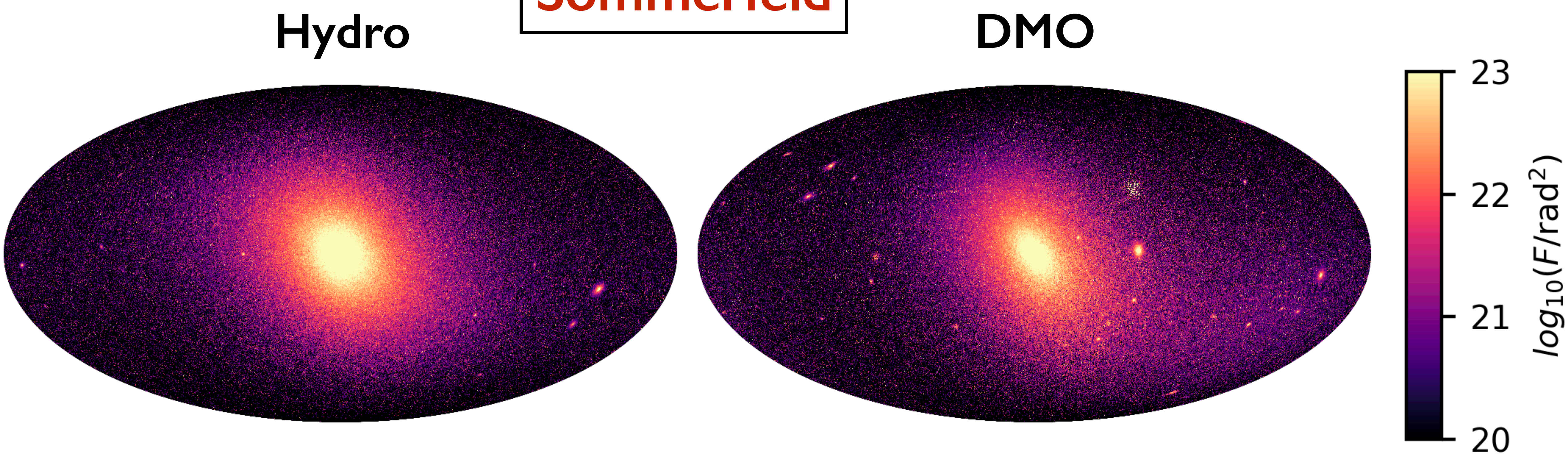

Piccirillo, Blanchette, **NB** et al, 2203.08853

- If we extrapolate the DM subhalos down to $\sim 1\,\mathrm{M}_{\odot}$, we find that subhalos dominate the smooth component beyond $\sim 0.2\, r_{200}$.

Dwarf spheroidal analogues

- Study the J-factors of Milky Way dSph analogues in APOSTLE.

Dwarf spheroidal analogues

- Study the J-factors of Milky Way dSph analogues in APOSTLE.
→ The DM relative velocity distributions of the dSphs agree well with a **Maxwellian distribution** at all radii.

Dwarf spheroidal analogues

- Study the J-factors of Milky Way dSph analogues in APOSTLE.
  → The DM relative velocity distributions of the dSphs agree well with a **Maxwellian distribution** at all radii.

- Simple **power-law relation** between the the Maxwellian peak speed and the maximum circular velocity of the dSph.

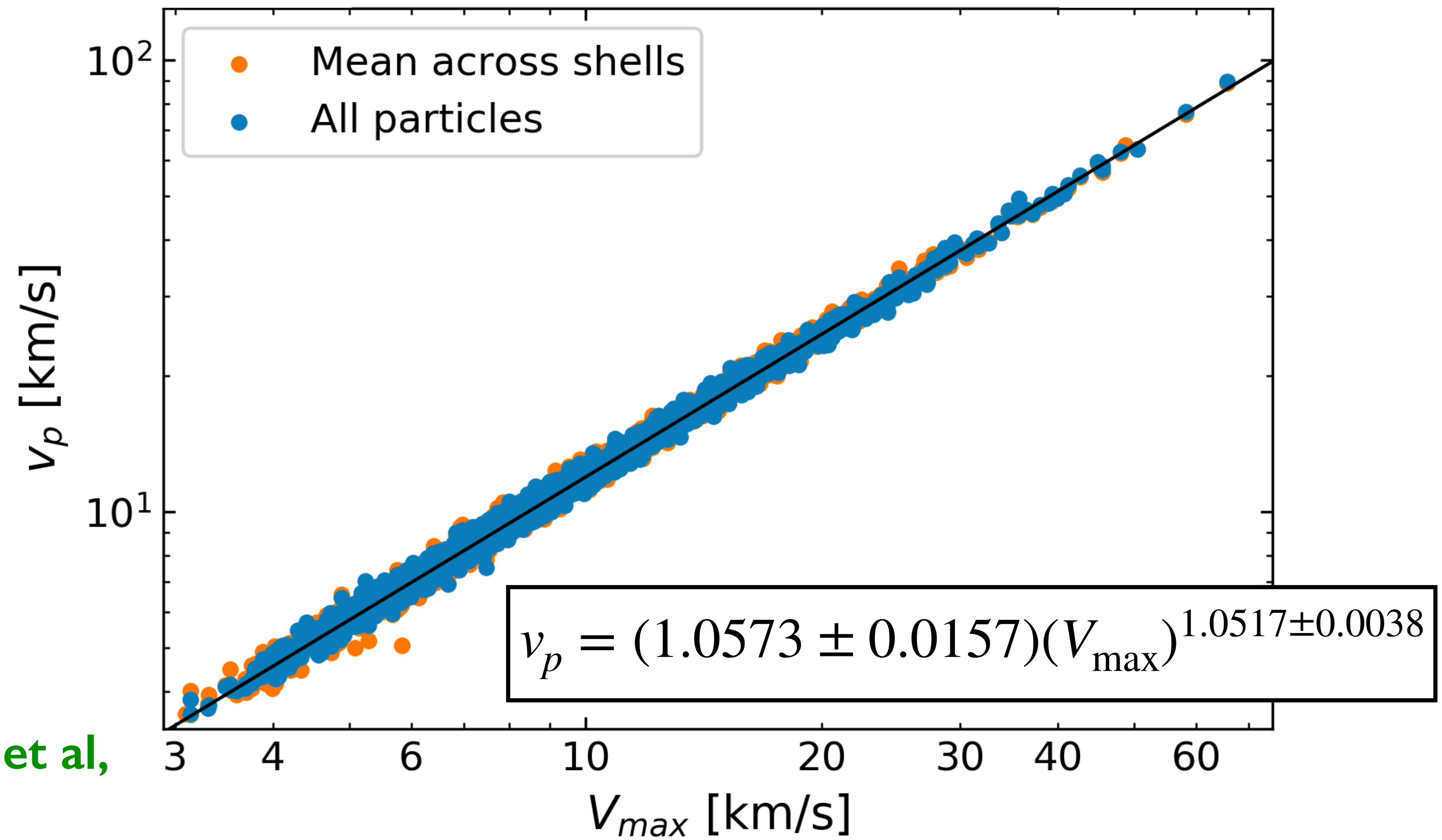

Blanchette, Piccirillo, NB et al, 2207.00069

Dwarf spheroidal analogues

- Study the J-factors of Milky Way dSph analogues in APOSTLE.
  → The DM relative velocity distributions of the dSphs agree well with a **Maxwellian distribution** at all radii.

- Simple **power-law relation** between the the Maxwellian peak speed and the maximum circular velocity of the dSph.

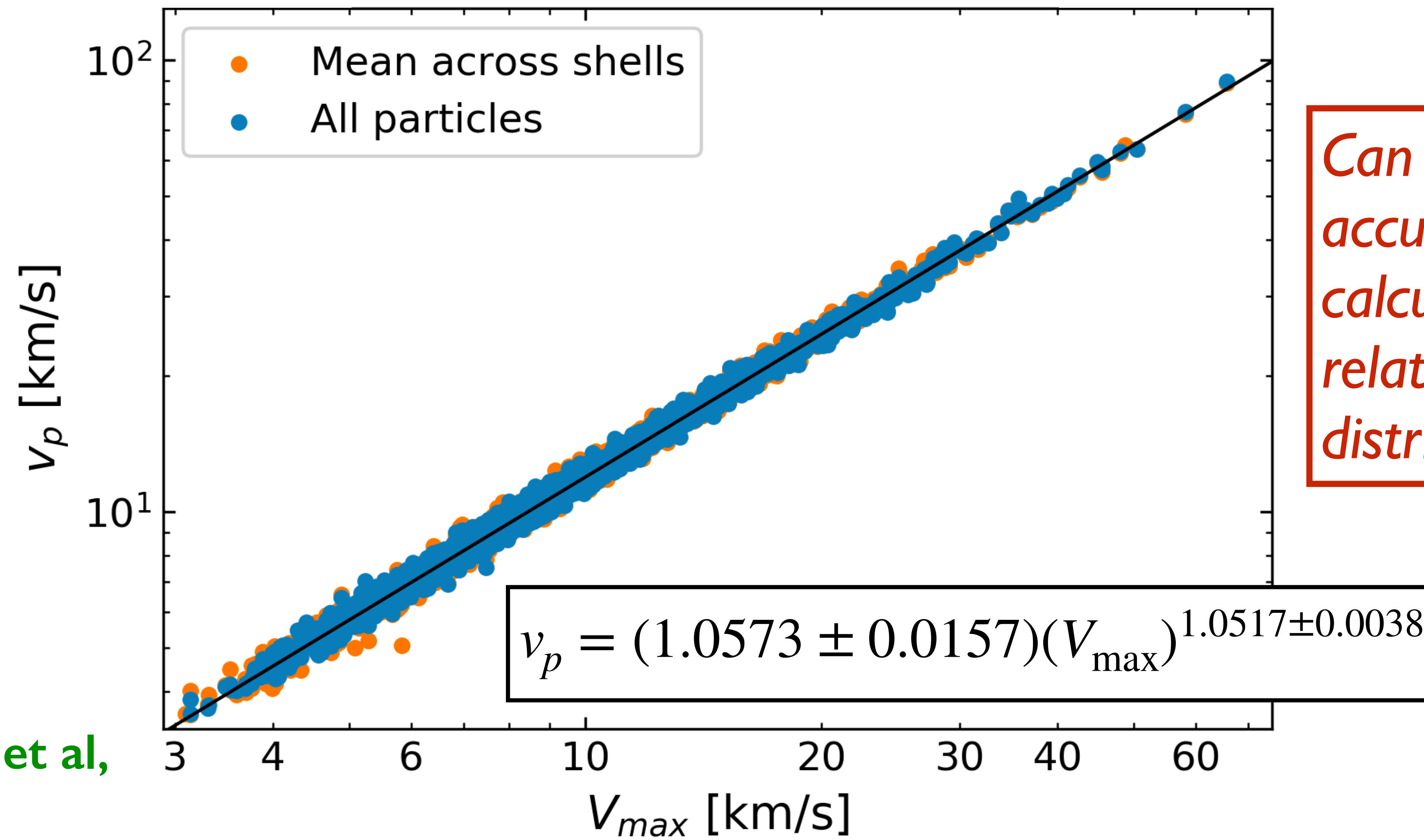

Can be used to accurately calculate the DM relative velocity distribution.

Blanchette, Piccirillo, NB et al, 2207.00069

Dwarf spheroidal analogues

- J-factors in good agreement with previous work which used simplified models for the DM velocity distribution.

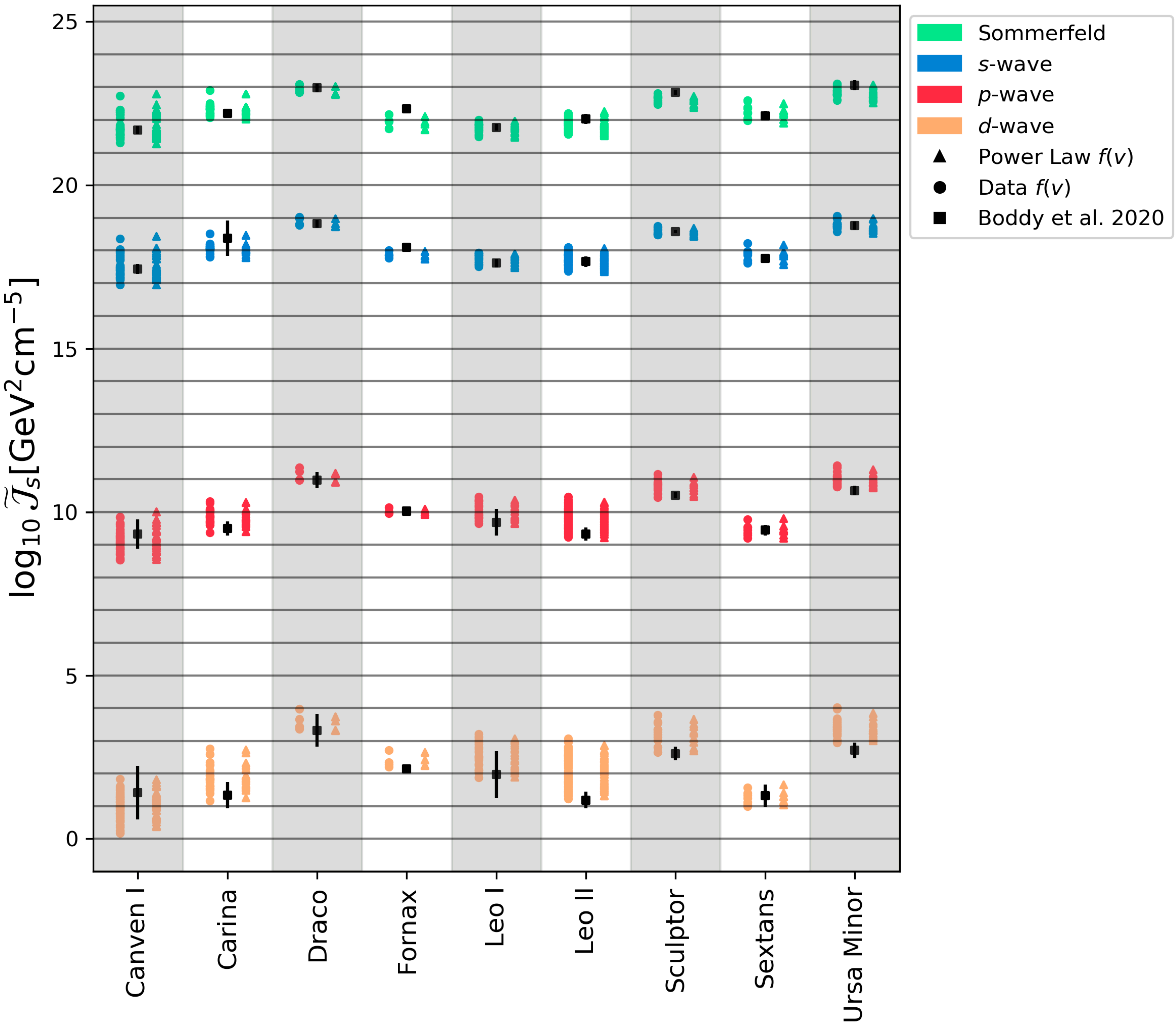

Blanchette, Piccirillo, **NB** et al, 2207.00069

Dwarf spheroidal analogues

- J-factors in good agreement with previous work which used simplified models for the DM velocity distribution.
- Halo-to-halo scatter in the J-factors dominate the astrophysical uncertainties.

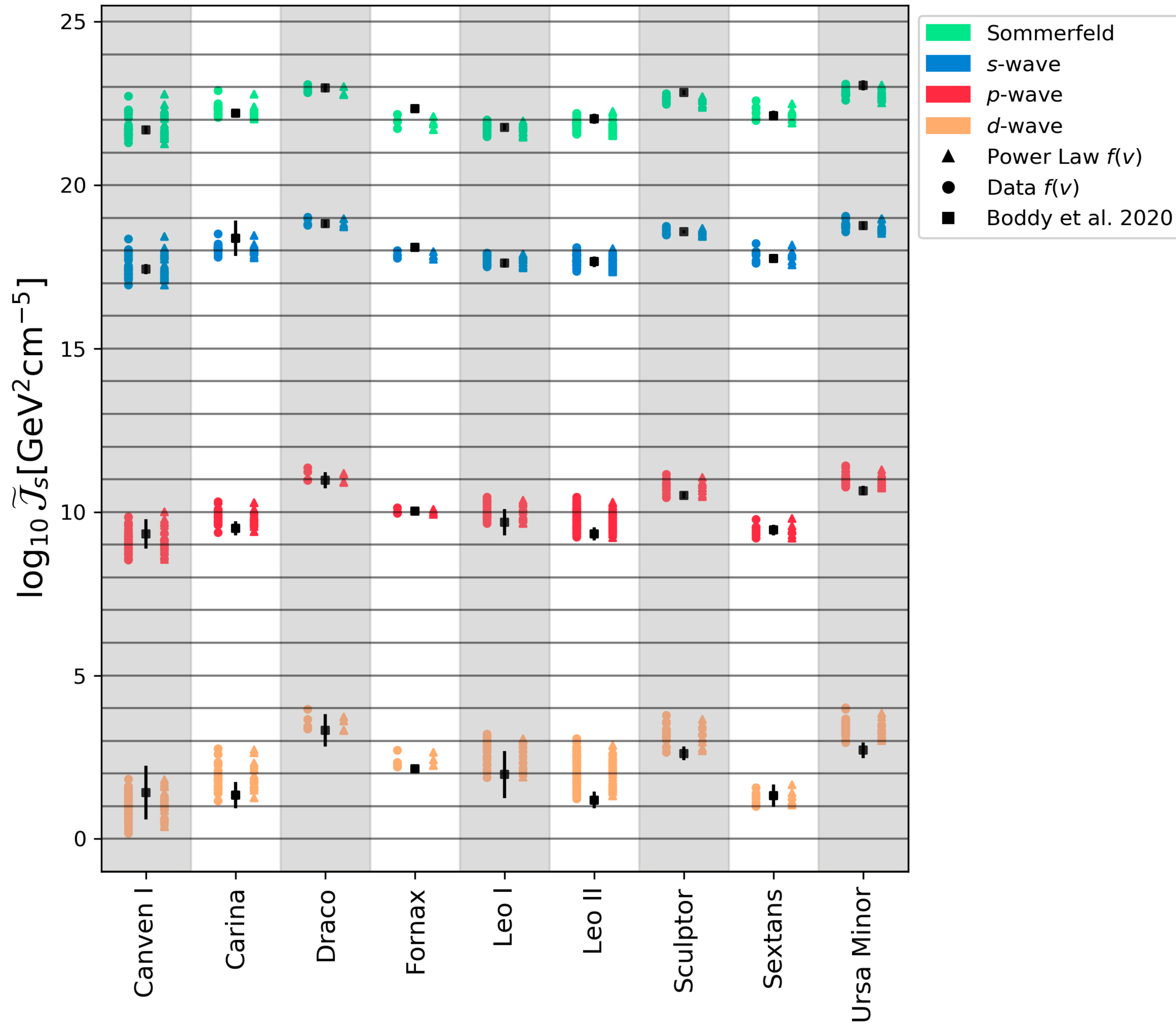

Blanchette, Piccirillo, **NB** et al, 2207.00069

Summary

- Cosmological simulations crucial for the interpretation of indirect detection signals in velocity-dependent models.

Summary

- Cosmological simulations crucial for the interpretation of indirect detection signals in velocity-dependent models.
- The DM relative velocity distribution in both the smooth halo and subhalos consistent with the Maxwellian distribution at all radii.

Summary

- Cosmological simulations crucial for the interpretation of indirect detection signals in velocity-dependent models.
- The DM relative velocity distribution in both the smooth halo and subhalos consistent with the Maxwellian distribution at all radii.
- J-factors strongly correlated with the DM density profile. → The DM annihilation signal can be accurately predicted if the density profile can be robustly determined.

Summary

- Cosmological simulations crucial for the interpretation of indirect detection signals in velocity-dependent models.

- The DM relative velocity distribution in both the smooth halo and subhalos consistent with the Maxwellian distribution at all radii.

- J-factors strongly correlated with the DM density profile. → The DM annihilation signal can be accurately predicted if the density profile can be robustly determined.

- Substructure most significant in Sommerfeld models.
  → Extrapolation down to lower subhalo masses important.

Summary

- Cosmological simulations crucial for the interpretation of indirect detection signals in velocity-dependent models.
- The DM relative velocity distribution in both the smooth halo and subhalos consistent with the Maxwellian distribution at all radii.
- J-factors strongly correlated with the DM density profile. → The DM annihilation signal can be accurately predicted if the density profile can be robustly determined.
- Substructure most significant in Sommerfeld models.
  → Extrapolation down to lower subhalo masses important.
- For Milky Way dSphs, a simple power-law (v_p - $V_{\rm max}$) can be used to accurately model the DM velocity distribution and calculate the annihilation signal.

Backup Slides

Relative velocity moments

- Moments of the relative velocity distribution:

$$\langle \sigma_A v_{\rm rel} \rangle (\mathbf{x}) \propto \int \mathrm{d}^3\mathbf{v}_{\rm rel} P_{\mathbf{x}}(\mathbf{v}_{\rm rel}) v_{\rm rel}^n \equiv \mu_n(\mathbf{x})$$

- For different DM annihilation models, $\langle \sigma_A v_{\rm rel} \rangle$ is proportional to:
  - **Sommerfeld**: Inverse moment μ_{-1}
  - **s-wave**: zeroth moment, $\mathcal{J}_s = \int d\ell \, [\rho(r(\ell, \Psi))]^2$
  - **p-wave**: 2nd moment → square of the relative velocity dispersion of the system at a given $\mathbf{x}$.
  - **d-wave**: 4th moment. Related to the kurtosis:

$$\kappa(\mathbf{x}) = \frac{\int d^3\mathbf{v}_{\rm rel} v_{\rm rel}^4 P_{\mathbf{x}}(\mathbf{v}_{\rm rel})}{\left[\int d^3\mathbf{v}_{\rm rel} v_{\rm rel}^2 P_{\mathbf{x}}(\mathbf{v}_{\rm rel})\right]^2} = \frac{\mu_4(\mathbf{x})}{(\mu_2(\mathbf{x}))^2}$$

Depends on the more extreme tails of the relative velocity distribution

Relative velocity moments

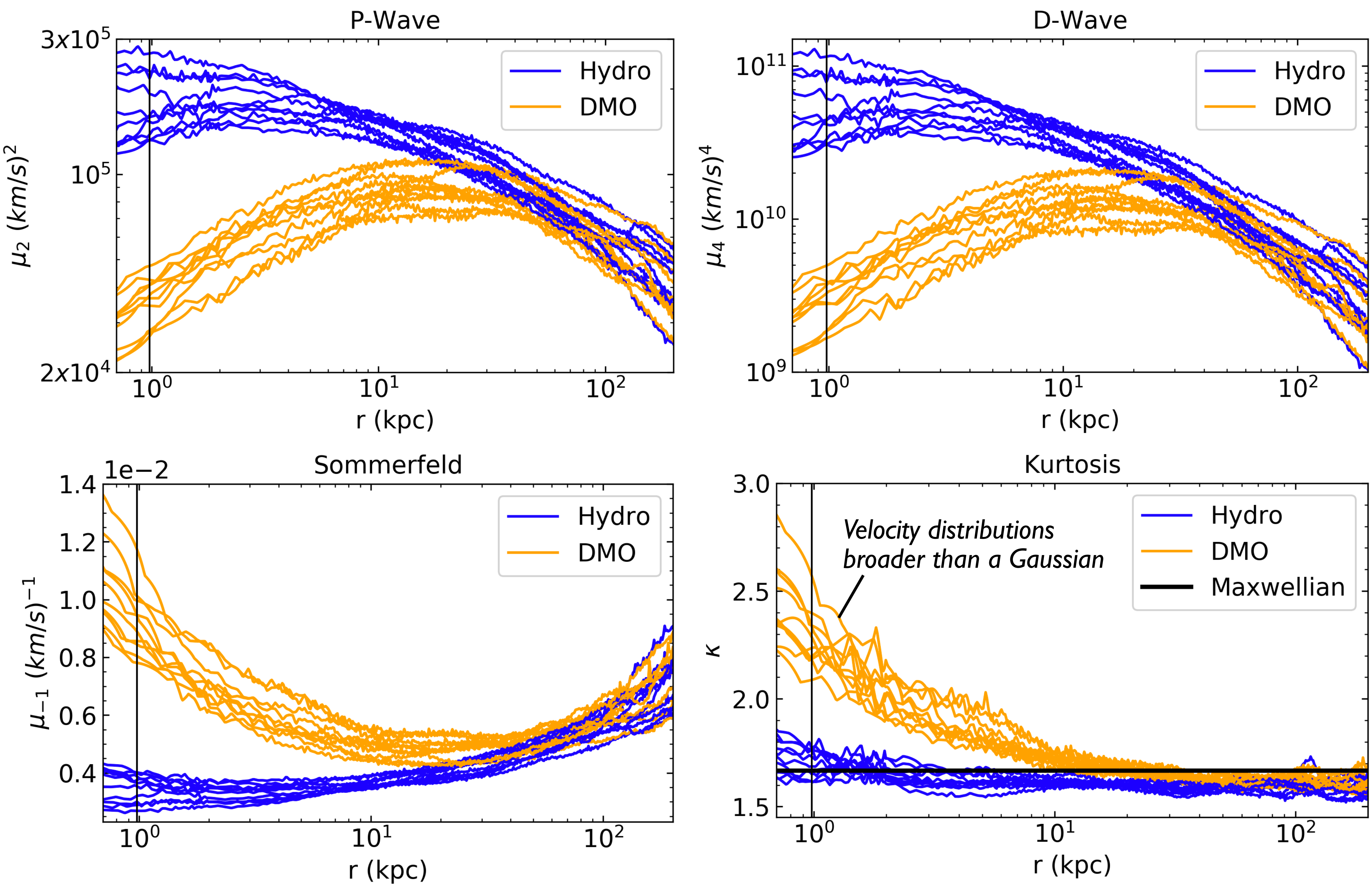

Board, **NB**, Strigari et al, 2101.06284

Effective J-factors

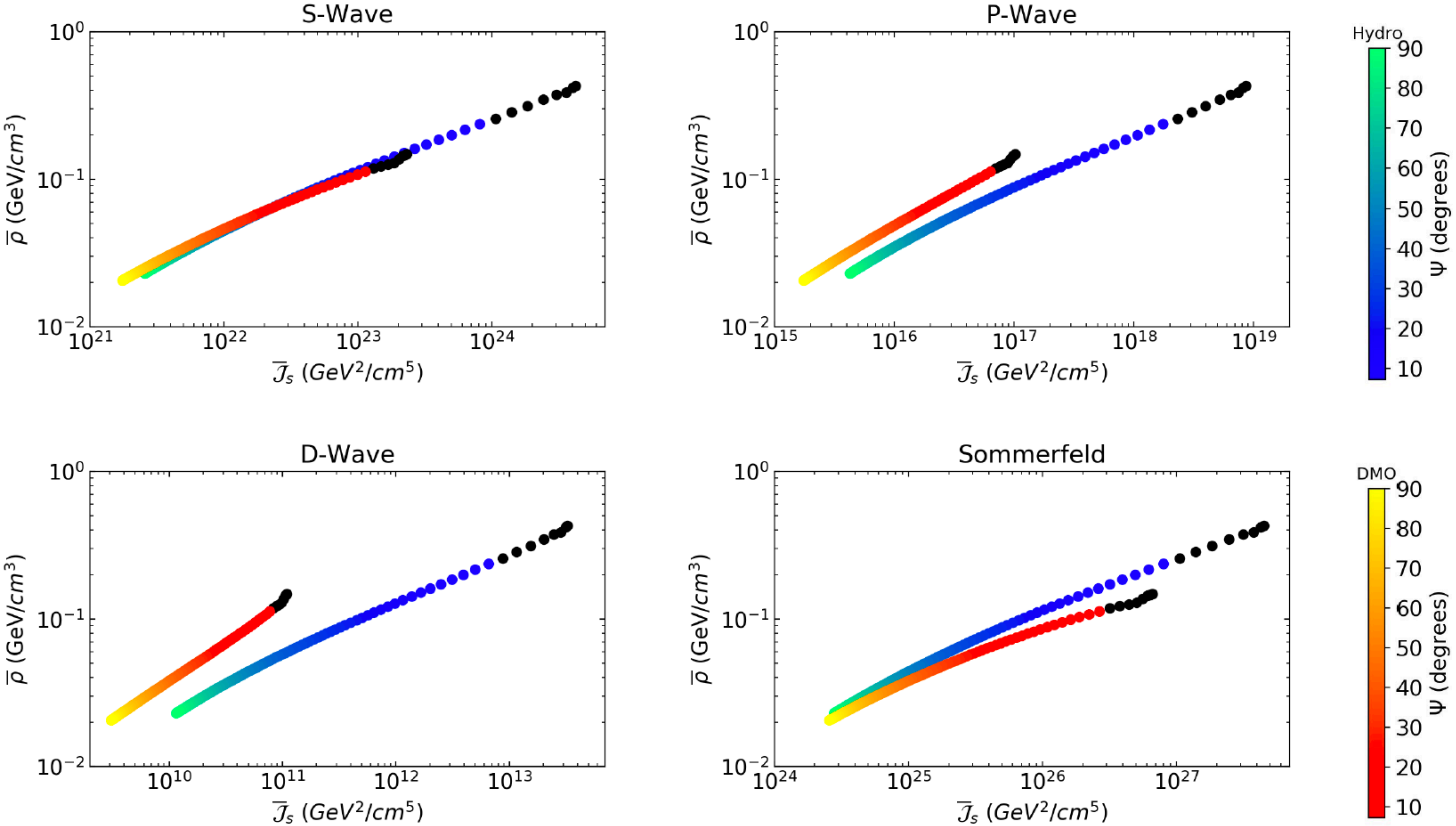

Board, **NB**, Strigari et al, 2101.06284

Effective J-factors

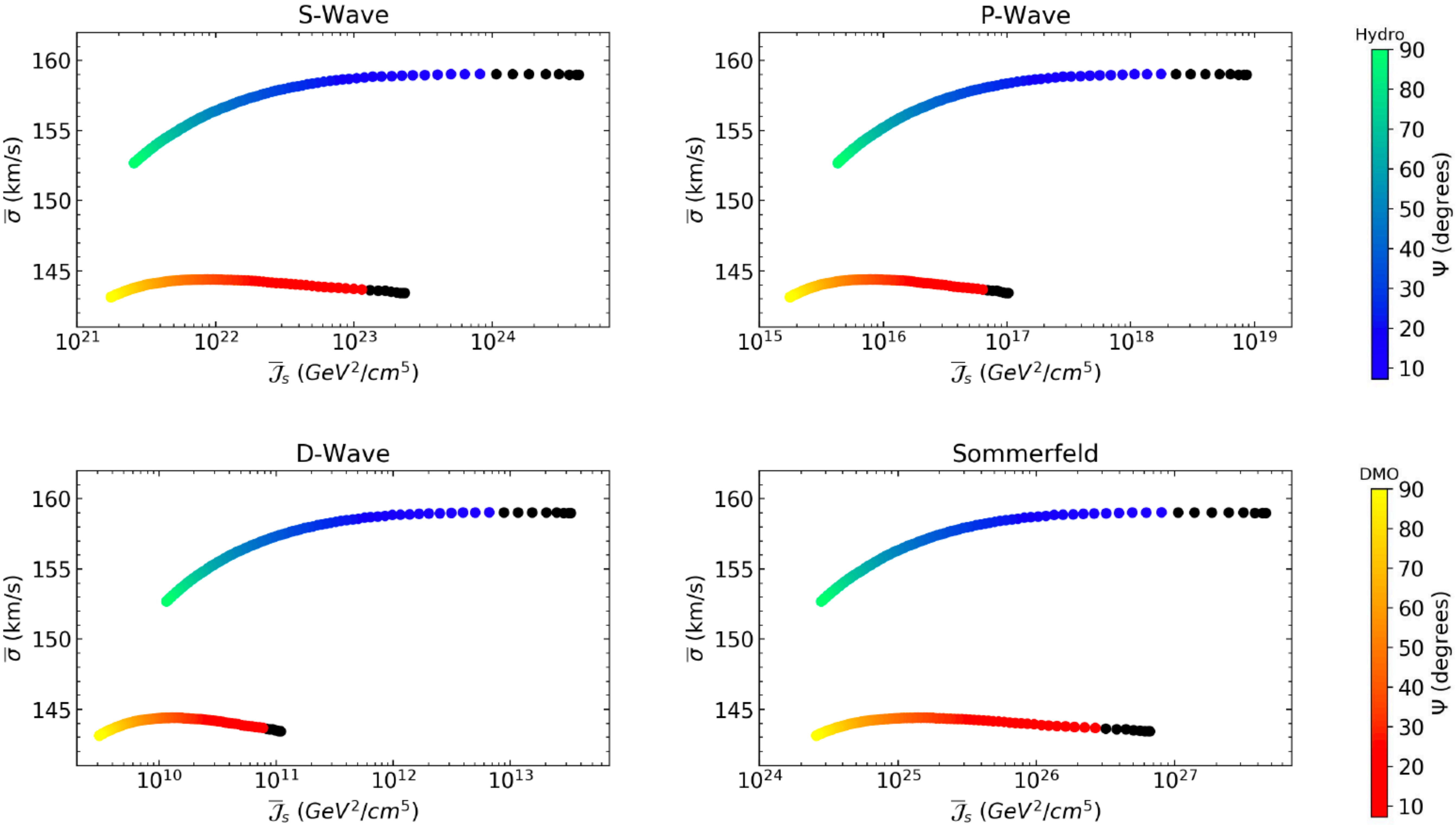

Board, NB, Strigari et al, 2101.06284

High resolution simulations

Auriga Simulations

Six high resolution halos.

Resolve subhalos with mass $> 10^6\,\mathrm{M}_\odot$

m_{DM} [$\mathrm{M}_\odot$]	m_{b} [$\mathrm{M}_\odot$]	ϵ [pc]
5×10^4	6×10^3	184

APOSTLE Simulations

Ten high resolution halos.

m_{DM} [$\mathrm{M}_\odot$]	m_{g} [$\mathrm{M}_\odot$]	ϵ [pc]
5×10^4	1.0×10^4	134

Cumulative number of subclass

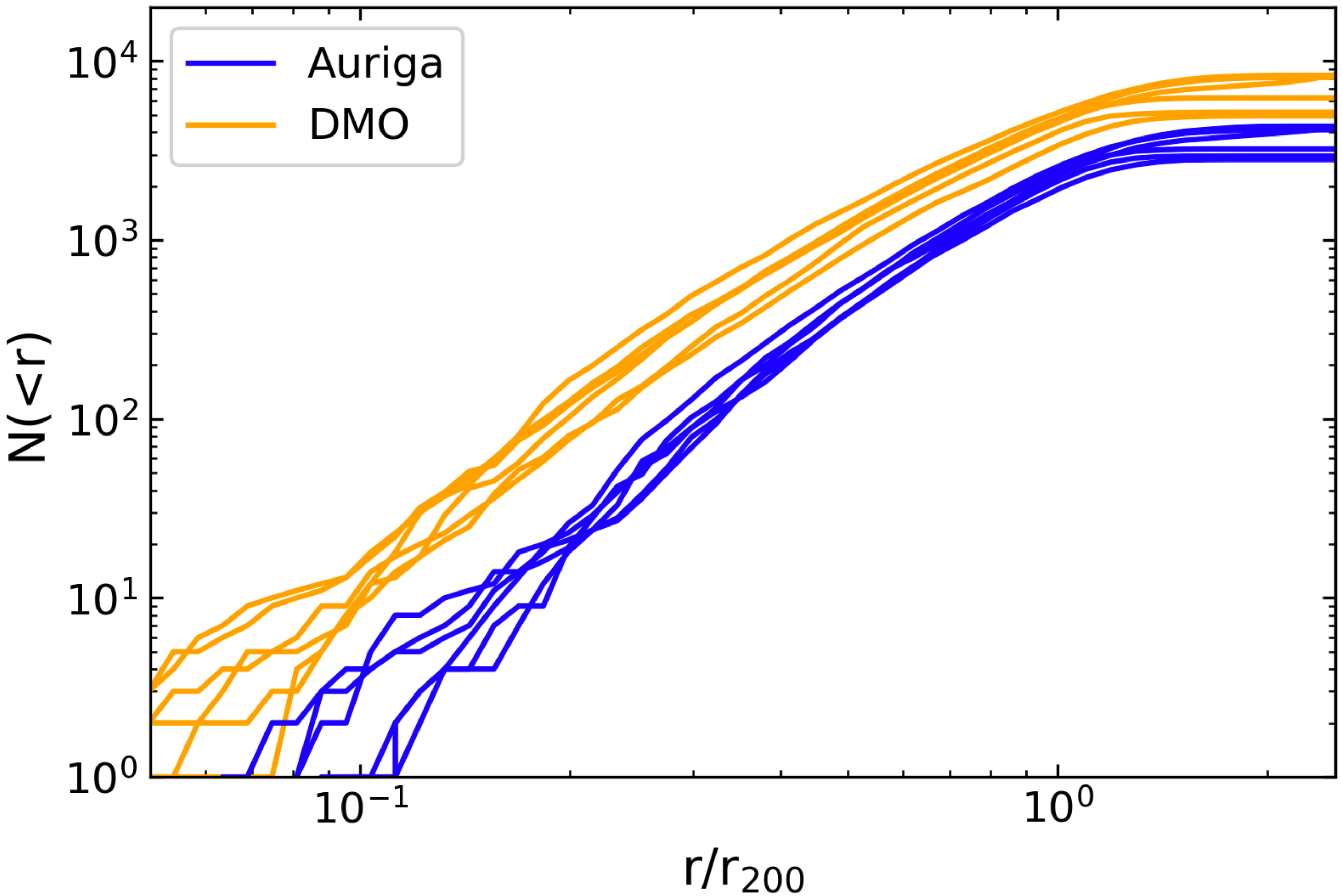

Piccirillo, Blanchette, **NB** et al, 2203.08853

Dark matter annihilation luminosity

- The annihilation luminosity from DM particles in some region of space can be written as

$$L_n = \int \mathrm{d}^3\mathbf{x} \int \mathrm{d}^3\mathbf{v}_{\mathrm{rel}} P_{\mathbf{x}}(\mathbf{v}_{\mathrm{rel}}) \left(\frac{v_{\mathrm{rel}}}{c}\right)^n [\rho(x)]^2$$
$$= \int \mathrm{d}^3\mathbf{x}\, [\rho(x)]^2 \left(\frac{\mu_n(\mathbf{x})}{c^n}\right)$$

- Use a Voronoi tessellation method to estimate the DM density at the location of each DM particle, from the DM particle mass and the cell volume surrounding the DM particle.

- Calculate the relative velocity distribution at each point on a spherical grid, using nearest 500 particles.

Dark matter annihilation luminosity

- For small subhalos, whose angular size <1 degree as seen from the Solar position, estimate the DM annihilation luminosity from a spherical region interior to $R_{\rm max}$:

$$L_{\rm sub} = \frac{C_{\rm Einasto} V_{\rm max}^4}{G^2 R_{\rm max}}$$

$$\begin{aligned} L_{n,{\rm sub}} &= \left(\frac{\mu_n}{c^n}\right) \int {\rm d}^3\mathbf{x}\, [\rho(x)]^2 \\ &= \left(\frac{\mu_n}{c^n}\right) L_{\rm sub} \\ &= \left(\frac{\mu_n}{c^n}\right) \left(\frac{C_{\rm Einasto} V_{\rm max}^4}{G^2 R_{\rm max}}\right) \end{aligned}$$

$$C_{\rm Einasto} = 1.87$$

- The annihilation flux: $F = L/d^2$ → heliocentric distance of the subhalo

Dark matter annihilation luminosity

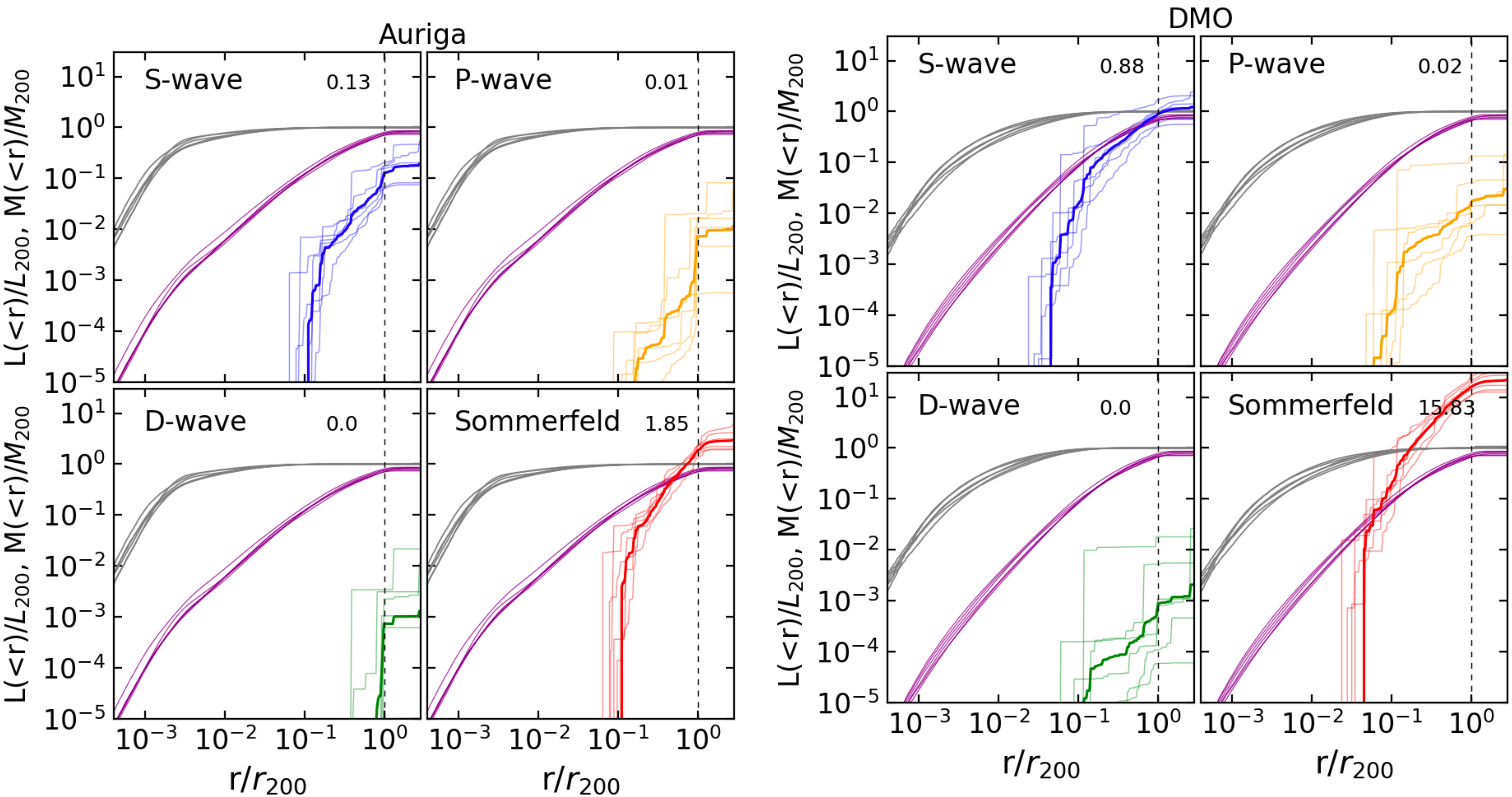

Piccirillo, Blanchette, **NB** et al, 2203.08853

Dark matter annihilation luminosity

Including extrapolated subhalos down to $\sim 1\,\mathrm{M}_\odot$

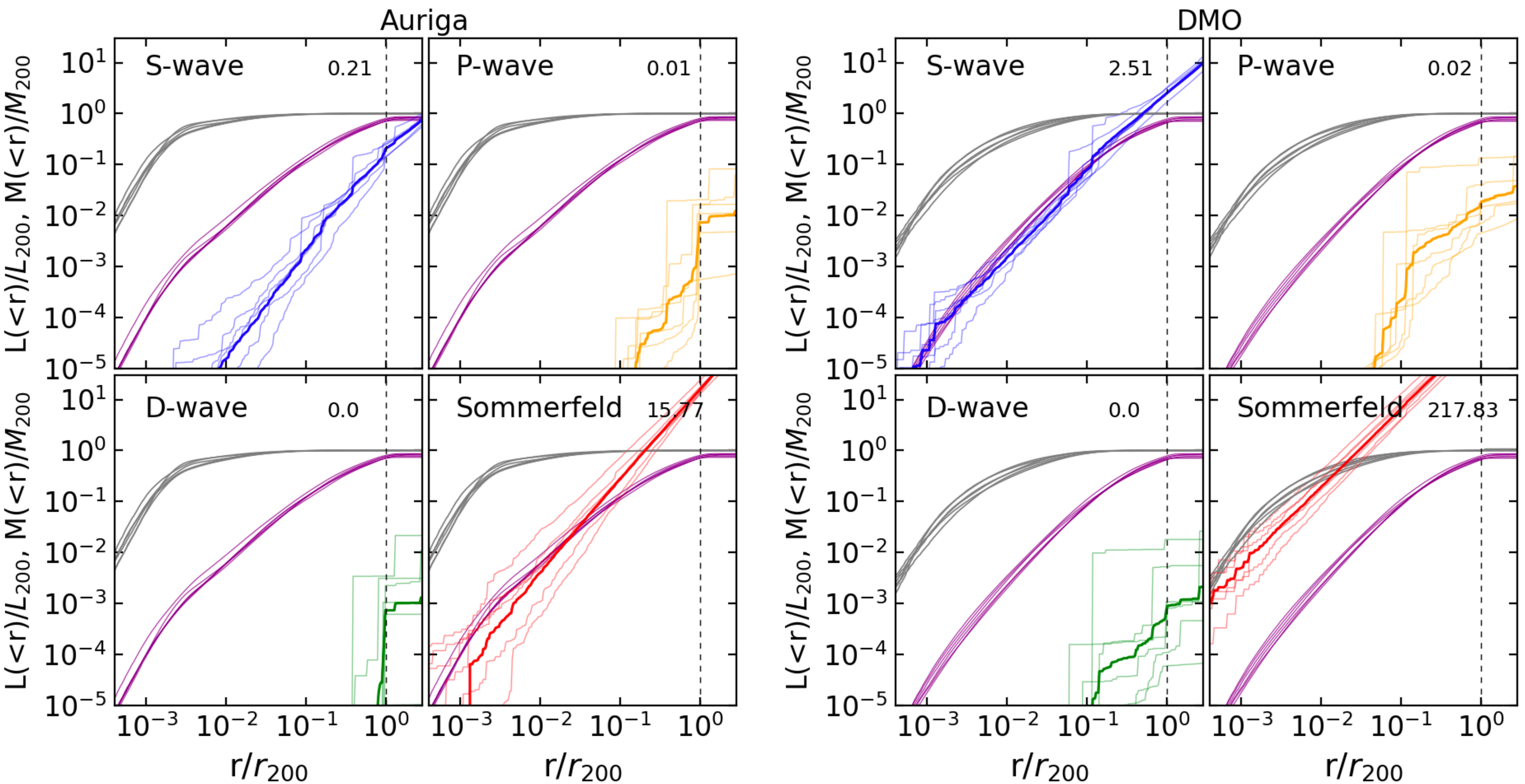

Piccirillo, Blanchette, **NB** et al, 2203.08853

Dwarf spheroidal analogues

dSph Analogue	N	$M_\star^{obs}$ [$M_\odot$]	$M_\star$ [$M_\odot$]	$V_{1/2}^{obs}$ [km/s]	$V_{1/2}$ [km/s]	V_{max} [km/s]	$\log_{10}(\tilde{\mathcal{J}}_s)$ [$GeV^2\,cm^{-5}$]
Canes Venatici I (1)	39	2.3×10^5	5.66×10^5	13.2	14.56	15.39	17.43
Canes Venatici I (2)			3.45×10^5		14.53	16.07	17.44
Carina (1)	23	4.3×10^5	2.38×10^5	11.1	11.30	13.14	18.52
Carina (2)			1.61×10^6		11.78	16.87	18.21
Draco (1)	4	2.2×10^5	8.91×10^5	17.5	14.92	24.32	18.81
Draco (2)			4.70×10^5		15.24	24.35	18.77
Fornax (1)	4	1.7×10^7	1.36×10^7	18.5	18.79	20.38	18.01
Fornax (2)			1.20×10^7		18.36	21.96	17.87
Leo I (1)	20	5.0×10^6	3.27×10^6	15.6	15.24	20.37	17.63
Leo I (2)			3.52×10^6		15.15	24.81	17.64
Leo II (1)	52	7.8×10^5	1.45×10^6	11.4	12.15	20.13	17.66
Leo II (2)			4.97×10^5		12.31	22.01	17.65
Sculptor (1)	11	2.5×10^6	6.10×10^6	15.6	15.73	27.27	18.56
Sculptor (2)			3.27×10^6		15.04	20.37	18.54
Sextans (1)	7	5.9×10^5	4.58×10^5	12.3	12.85	13.02	17.70
Sextans (2)			1.58×10^6		12.91	12.98	17.87
Ursa Minor (1)	24	3.9×10^5	9.30×10^5	19.9	19.37	24.41	18.75
Ursa Minor (2)			7.79×10^5		18.41	25.97	18.75

J-factor for Carina analogue

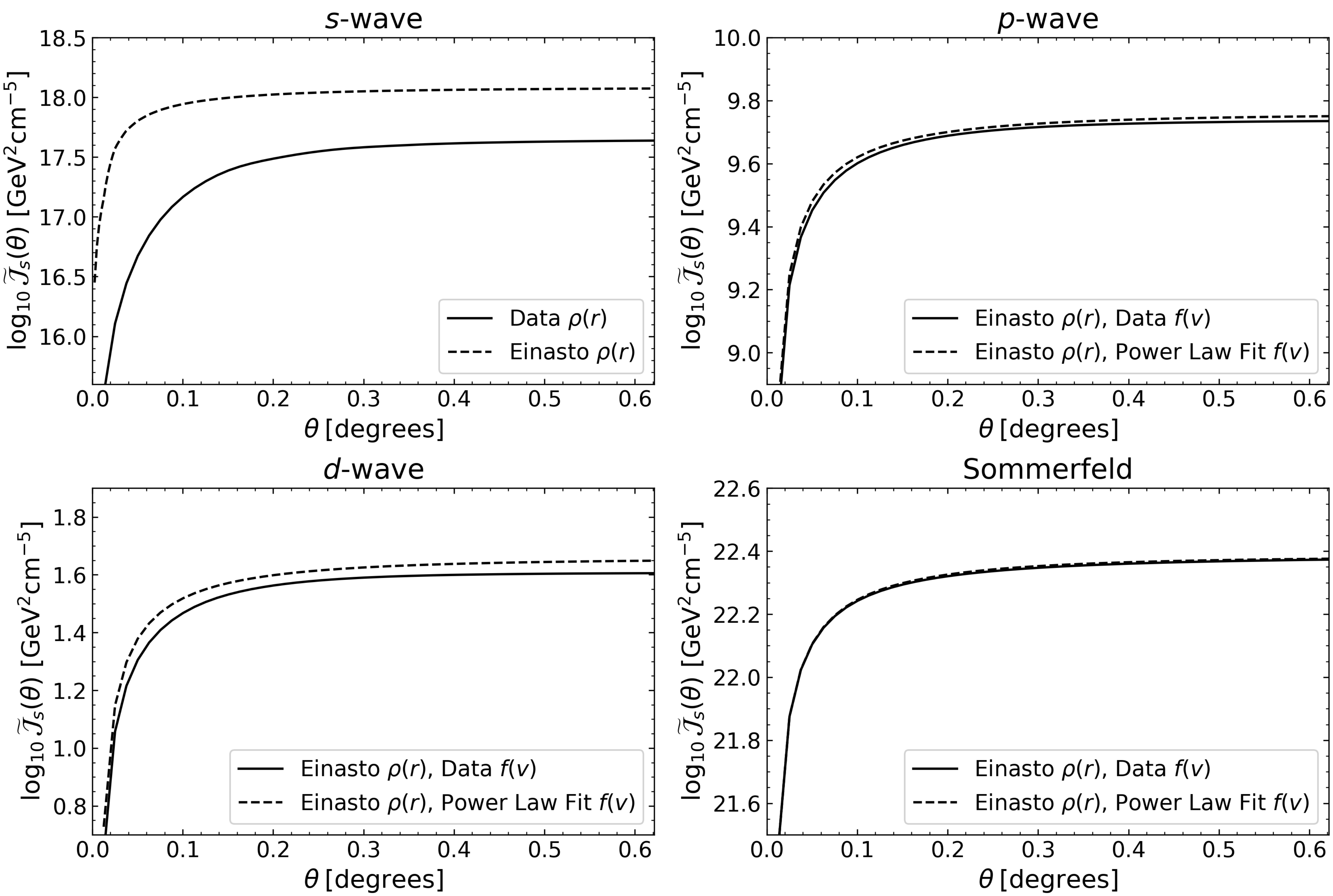

Comparison to Maxwellian

- The errors introduced in the J-factors if we model the relative velocity distribution of the dSph as a Maxwellian are small.
- Using the power-law relation introduces an error of ~13% in the J-factors.